THE UNIVERSITY OF MICHIGAN

INDUSTRY PROGRAM OF THE COLLEGE OF ENGINEERING

THE INFLUENCE OF SOME PHYSICAL PROPERTIES ON MACHINABILITY OF METALS

Alexander Henkin

A dissertation submitted in partial fulfillment
of the requirements for the degree of
Doctor of Philosophy in the
University of Michigan
Department of Mechanical Engineering
1962

June, 1962

IP-572

Doctoral Committee:

Associate Professor Joseph Datsko, Chairman
Professor John A. Clark
Professor Samuel K. Clark
Professor Charles Lipson
Professor Clarence A. Siebert

ACKNOWLEDGEMENTS

I wish to express my appreciation to:

Professor J. Datsko, the Chairman of the Doctoral Committee, for his encouragement, critical suggestion and friendly counsel.

Professors J. A. Clark, S. K. Clark, C. Lipson and C. A. Siebert, Members of the Doctoral Committee, for their advice and assistance during this investigation.

Professor J. G. van Wylen, Chairman of the Mechanical Engineering Department for my staff appointment, and the H.T.I and Rackham School of Graduate Studies for the Predoctoral fellowships.

The other members of the staff for their constructive comments.

The National Science Foundation for its financial support of this study.

The United Steel Corporation, the Bethlehem Steel Company, the Aluminum Company of America and the Climax Molybdenum Company of Michigan for the materials provided for this research.

The Industry Program of the College of Engineering for its help in the reproduction of the dissertation.

TABLE OF CONTENTS

LIST OF TABLES

LIST OF FIGURES

LIST OF FIGURES (CONT'D)

I. INTRODUCTION

In response to the increased commercial interest in maching operations in the middle of the last century, the first scientific approach to the art of metal cutting was initiated. Theory kept pace with practice up to the invention of the High Speed Steel by Taylor and White in 1898. With this discovery, the art of metal cutting entered an "Empirical Period," which was not brought to an end by any of the later scientific works. This latter period yielded empirical relationships between cutting conditions, tool life, cutting forces, power requirement and surface finish.

Despite the large number of attempts to analyze the cutting process, basic relationships between the physical properties and the process variables are lacking. This is all the more disappointing as the behavior of the materials in other processes, like forming, welding and heat treatment is fairly well predictable.

Though, strictly speaking, metal cuttting is a three dimensional operation, it approaches a two dimensional process for some particular cases. Most of the analytical studies of metal cutting were directed to study the idealized, orthogonal, two dimensional cut. With all its simplification, the prediction of the behavior of a metal, even in the two dimensional cut, has been beyond our present day's knowledge. This is not surprising, considering the state of the theory of plasticity, and the limited understanding of the friction and wear phenomena. The metal cutting researchers have further restricted their studies mainly to the formation of a continuous chip in the absence of a built-up-edge.

Figure 1 shows the three types of chips as classified by Ernst.[1] It should be mentioned that the difference between them is not as distinct as the micrographs may suggest.

Figure 2 demonstrates the force and chip geometry for the idealized two dimensional cutting process. An orthogonal cutting tool, with a rake angle α, is removing a layer of depth t and width w from a given work piece. If $t \ll w$ then the operation is essentially a plane strain process. The operation, a plastic forming process, is classically idealized by assuming shear to occur along a shear plane, defined by its shear angle ϕ. The force R acting on the tool could be resolved either into the cutting force F_H and the feeding force F_V, or into the tangential component F and the normal component N. The ratio between the last two components is defined as the coefficient of friction μ; $\mu = F/N = \tan\beta$, where β is the friction angle. The reaction R', equal and opposite to R is resolved into a shearing force F_s, acting along the shearing plane, and a force F_n, acting normal to the shearing plane. To complete the description of Figure 2, we have to introduce the chip ratio r, defined as $r = t/t_c$, where t_c is the chip thickness.

An innumerable number of attempts has been made to predict the shear angle, chip ratio, coefficient of friction, etc., but unfortunately with very little success. Data obtained experimentally, could in many cases be correlated reasonably well for one set of conditions, but the relationships derived had no general validity. In any machinability study the researcher has always had to resort to measurement of some of the values mentioned above, and then compute the others from geometrical considerations.

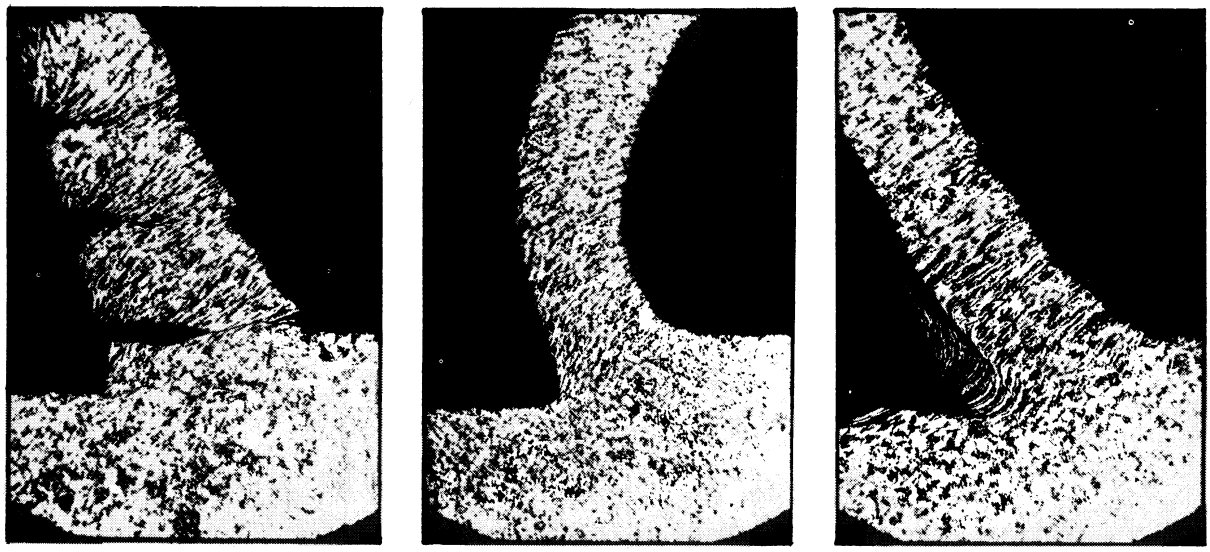

Figure 1. The Three Basic Chip Types According to Ernst[1]. Type 1, Discontinuous or Segmental Chip; Type 2, Continuous Chip Without Built-Up Edge; and Type 3, Continuous Chip with Built-Up Edge.

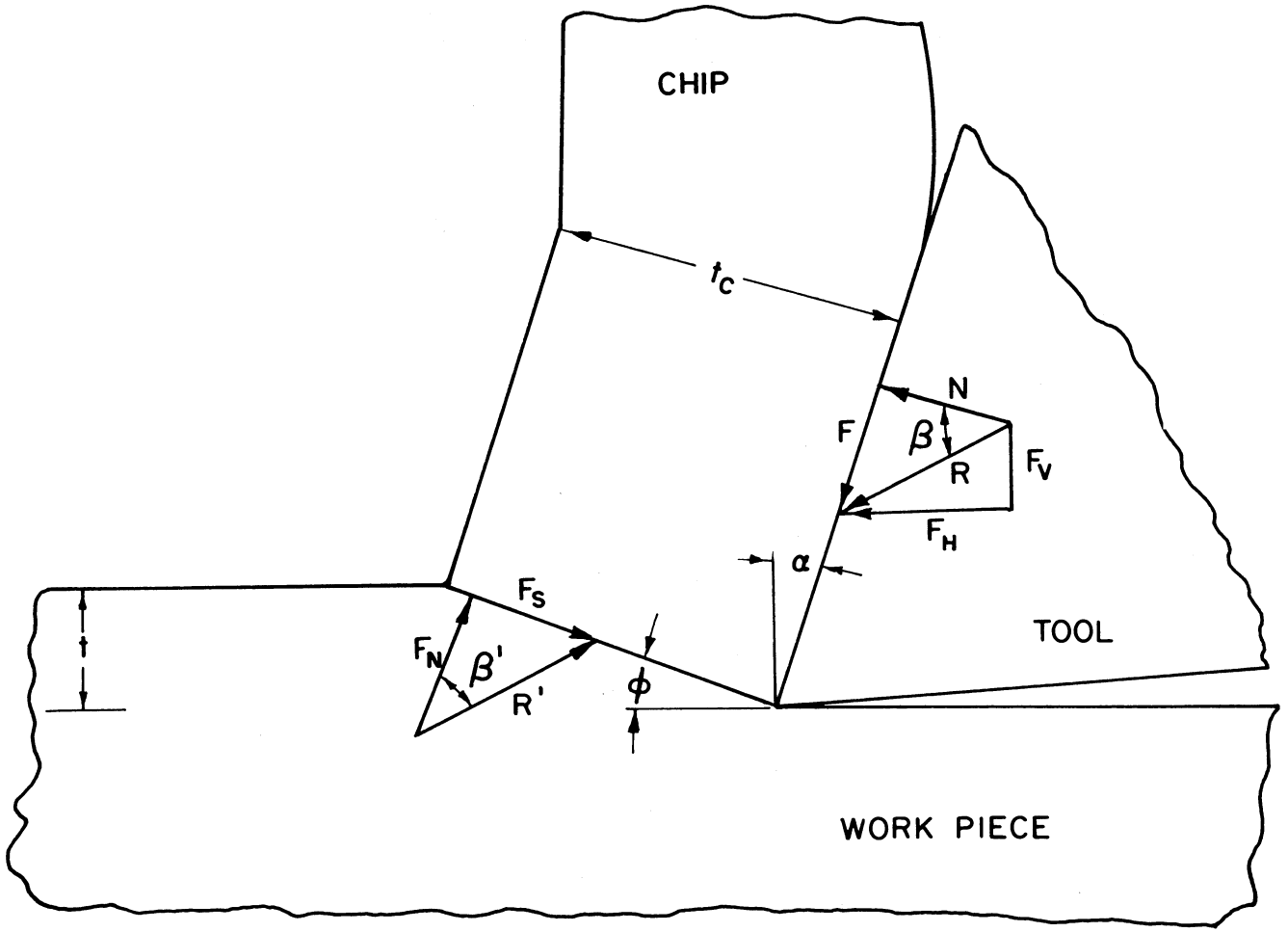

Figure 2. Force Chip Geometry for an Idealized Two Dimensional Cut.

By machinability the engineer invariably refers to the relative "ease" with which a material can be worked in a chip forming process. Among the extremely different criteria applied to evaluate machinability are: tool life, surface finish, forces, power consumption and dimensional stability. The tool life as a criterion for machinability is of most general significance, though the other criteria may be of equal importance for some special conditions. The standard machinability ratings[2], referred to sometimes as machinability indexes, are comparisons of the relative cutting velocity of the work material with the cutting velocity of a standard material for some specific cutting conditions. Free machining steel, AISI 1112 or 1212, is used most often as the standard for ferrous materials. Because of its importance, the tool life criterion was adopted in this study.

The factors affecting the machinability are the tool, the cutting conditions and the work material. All of these factors have attracted the attention of the metal cutting researchers for more than a hundred years. But, as Optiz[3] stated in 1960, "In spite of the abundance and diversity of the material, it is not possible up to the present to make positive predictions concerning tool life values of various materials."

The objective of this investigation was to study both analytically and experimentally the effect of the physical properties of the work material on machinability. Among the physical properties studied were the stress strain relations, hardness, microstructure, abrasiveness and the thermal properties. A variety of materials, ferrous and non-ferrous, was selected to insure the largest possible variation in each one of the physical properties. All of the variables except the work material and the speed-tool

life relationship for a set of standard cutting conditions were fixed for two reasons: first, it was not the intention of this investigation to study the effect of the tool and the cutting conditions on machinability, and secondly, sufficient experimental data is already available in the literature.

II. LITERATURE REVIEW

General

Whereas the machining process as such can be traced back to the earliest stages of civilization, the actual scientific approach to the art of metal cutting did not start until the turn of the nineteenth century. It was with Rumford[4], who presented in 1798 to the Royal Society of London his paper on an "Inquiry Concerning the Source of Heat Which is Excited by Friction," that this period started. Rumford attempted to show, by measuring the temperature rise in a canon boring process, that a change in heat capacity is associated with the formation of chips. Considering that fifty years were to pass before Joule introduced the concept of the "mechanical equivalent of heat," it is not at all surprising that Rumford could not successfully compute the work required for the chip formation from his temperature measurements.

It was not until 1851 that any further significant studies in metal cutting were published. In that year Cocquilhat[5], who was the first to measure cutting forces, measured drilling torques. From the experimental data he very carefully computed the cutting pressures and the specific work per unit volume required in a metal removal process. From here on the number of publications in the area of machining has been steadily increasing until at the present time the total number exceeds several thousands.

The effect of the cutting geometry on the efficiency of the cutting process was studied by Joessen.[6] His reports in the Austrian Engineering Journal in 1865 showed the studies of the drilling and the

turning operations. He concluded that a rake angle of 36° in turning, and an included angle of 70° in drilling minimized the cutting forces.

The greatest influence on the development of the machining processes had undoubtedly the invention of the high speed steel by Taylor and White in 1898. The vast experimental work carried out by Taylor was summarized in his 1907 ASME presidential address: "On the Art of Metal Cutting."[7] This classical reference, a summary of a lifelong work by Taylor, is one of the most extensive machinability research projects ever undertaken by an individual. His most interesting conclusion, universally accepted today, is the exponential relationship between the cutting velocity V and the tool life T_L, namely $VT_L^n = C$. In this equation, referred to as the Taylor relationship, C and n are constants the value of which depends on the cutting tool, the cutting conditions and the work material.

Chip Formation

The first attempts to explain the mechanics of chip formation are due to Timme[8,9,10] and Tresca[11,12]. Tresca, who has developed many of the most basic concepts of the theory of plasticity, has contributed two classical articles to the field of metal cutting. In his 1873 paper "Planing of Metals"[11], and in his 1878 paper "On Further Applications of the Flow of Solids"[12] he describes in detail the cutting process and the chip formation. Tresca considered the work material to be compressed in front of the tool, and then sheared in a plane parallel to the cutting direction. Though this observation is

incomplete, it seems to be partly true in the light of recent studies associated with this thesis made on polished and etched specimens and observed through a microscope during machining.

The second researcher, a contemporary of Tresca, who made some of the most basic contributions to the science of metal cutting was Timme. Timme was the first to recognize that the chip formation is the most basic aspect of metal cutting. He disagreed with Tresca on the mechanism of chip formation. Timme explained that the chip is formed by fracture along successive shear planes that are inclined to the direction of cutting. Though the writer disagrees with this explanation of the mechanics of the chip formation, credit should be given to Timme for his most excellent paper at such an early time of the development of both the theory of plasticity and the science of metal cutting.

Mallock[13] in 1881 presented to the Royal Society of London an excellent paper on the subject of metal cutting. He examined polished and etched chips, and concluded that the deformation is restricted to clearly defined shear planes, which are inclined at an angle ϕ to the cutting direction. Fracture occurs in these shear planes. Mallock was also the first to describe the chip formation in terms identical with the current "sliding deck of cards concept," that is often acknowledged as originating with Piispanen[14] in 1937 or Merchant[15] in 1945. He observed the effect of cutting fluids on friction but failed to note their effect on the shear angle.

Hartig[16] in 1873, Smith[17] in 1882, and Haussner[18] in 1892 were among the original contributors to the development of force and power measurement, so essential to the study of the metal flow. Though they all

measured only the component in the direction of the cutting velocity, Hausner already recognized that forces exist in other directions. Since these early investigations, force and power measurements became a standard procedure in machinability research, due in great part to Boston's work at the University of Michigan.

A controversy was raised by Reuleaux[19,20] in 1900 by suggesting that a crack develops ahead of the tool. This was also observed by Kingsbury[21] who commented on the same phenomenon. The work by Kick[22] in 1901, Brooks[23] in 1905 and Rosenhain[24] in 1906 negated this concept. The writer himself has observed many cracks propagating in front of the tool for various ductile materials during current work being done on the same project that sponsored this thesis.

Timme's work in Russia was followed by Briks[25] and Zvorikin[26]. As early as 1893 Zvorikin, by minimizing the cutting force, came up with the shear angle relationship:

$$\phi = 45 + \alpha/2 - \beta/2 - \beta'/2 \qquad (1)$$

Where ϕ is the shear angle, α the rake angle β the friction angle between the chip and the tool, and β' the friction angle in the shear plane. This relationship, for $\beta' = 0$ continued to appear as a new contribution, developed independently and sometimes on different postulates by various research workers for the past thirty years.

Hermann[27] in the 1896 edition of the "Lehrbuch der Ingenieur und Maschinenmechanik" derived the relationship

$$\phi = 45 + \alpha/2 - \beta/2 \qquad (2)$$

on the premise that the shear plane is that plane in which the shearing stresses are maximum. Linder[28] in 1907, Piispanen in 1937[14], Ernest and Merchant[29] in 1941 and again Merchant[15] in 1945 obtained the same relationship, and some of the aspects of their work will be discussed later.

It will be appropriate at this stage to interrupt the discussion of the chip formation and mention, in their historical order, the development of some of the more important tools of the metal cutting researcher, as well as some of the more interesting observations, carried out during the 1920's and 1930's.

The first persons to measure the chip temperature were Bruckenburg and Meyer[30] in 1911. Usacher[31] in 1915, was the first to actually measure the tool temperature by inserting thermocouples in the tool. But it was not until the middle of the twentites when Shore[32], Gottwein[33] and Herbert[34] published independently their work on tool chip interface temperature measurement by the tool-work thermocouple method. Extensive work in this area was carried out by Boston[35] and Schmidt[36], but it was not until the late 1940's that the problem was attacked analytically by Chao and Bisacre[37] Chao[38], Loewen[39] and others.

Coker[40,41] applied photoelasticity to the study of the stress distribution in the metal cutting process. Though it obviously could not reveal the stress distribution in the plastic region, it gave some interesting results about the nature of that region and the stresses around it. At the same time Schwerd[42] and Ishii[43] developed the techniques of photographing the cutting process in action, in contrast to the photomicrographs of the interrupted cut obtained earlier. Okochi and

Okoshi[44,45,46] were among the leaders of the metal cutting research in Japan, and employing some of the finest measuring and observation techniques they studied cutting forces, stress distributions, flow directions and the built-up edge problem.

Both Okoshi[46] in Japan and Schwerd[47] in Germany, related the built-up edge to the cutting velocity, whereas Rapatz[48] attributed it to the cutting temperature. Rapatz claimed that velocity effects the built-up edge only indirectly by effecting the temperature, and this was supported by elevated temperature cutting tests by Ernest and Martellotti[49]. During the same period Rosenhain and Sturney[50] have made their studies showing the built up edge to be part of the chip.

In 1937 Piispanen[14] established the shear angle graphically by minimizing the power requirement. Recognizing the effect of the normal force on the shear plane he modified his analysis respectively. His paper "Theory of Formation of Metal Chips," that appears in the J. App. Phys.[51] in 1948 sums up the same work analytically, and adds a study of the discontinuous chip formation.

Ernst and Merchant[29], obtained the expression for the average shearing stresses τ in the shear plane, referring to Figure 2 as:

$$\tau = \frac{F_s}{A_s} = \frac{F' \cos(\phi + \beta - \alpha)\sin\phi}{A} \qquad (3)$$

where A_s and A = wt are the area of the shear plane and the area of the cut respectively. Postulating that τ is maximum, by taking a derivative with respect to ϕ they obtained for the shear angle ϕ the same expression as in Equation (2). Obviously they assumed an independence between R' and β.

In 1945 Merchant[15] repeated his analysis following the same reasoning as Zvorikin, minimizing the power P, or the cutting force F_H given by

$$F_H = \frac{\tau A \cos(\beta - \alpha)}{\sin\phi \cos(\phi + \beta - \alpha)} \tag{4}$$

The results were again those of Equation (2). Merchant further refined his solution by introducing the effect of the normal stress σ on the shear stress τ.

$$\tau = \tau_o + K\sigma \tag{5}$$

where τ_o and K are constants. From Figure 2 it follows that

$$\sigma = \tau \tan(\phi + \beta - \alpha) \tag{6}$$

substituting Equation (6) in Equation (5) gives:

$$\tau = \tau_o + K\tau \tan(\phi + \beta - \alpha) \tag{7}$$

substituting the value of τ from Equation (7) into Equation (4) yields an expression for F_H

$$F_H = \frac{\tau_o A \cos(\beta - \alpha)}{\sin\phi \cos(\phi + \beta - \alpha) - K \sin\phi \sin(\phi + \beta - \alpha)} \tag{8}$$

Differentiating F_H with respect to ϕ as before, assuming the complete independence of the variables results in the shear angle relationship

$$\cot(2\phi + \beta - \alpha) = K \tag{9}$$

or

$$\phi = \frac{\alpha}{2} - \frac{\beta}{2} + C \tag{10}$$

where: C = arc cot K which Merchant called the "machining constant."

At a later date Merchant and Field[52] returned to study the mechanics of the discontinuous chip.

Stabler[53] on purely geometrical considerations obtained in 1951 the expression:

$$\phi = 45 - \beta + \alpha/2 \tag{11}$$

Lee and Shaffer[54] applied the methods of analyzing the stress and strain distributions in the plane plastic flow of an ideally plastic material to the problem of machining.

Figure 3 shows the slip line field associated with the appropriate boundary conditions, and the corresponding Mohr circle diagram. The region ABC is plastically rigid and under a uniform state of stress. If we substituted our notation for his, to say

$$\begin{aligned} w &\equiv \phi \\ \lambda_t &\equiv \beta \\ \gamma &\equiv \alpha \end{aligned} \tag{12}$$

we obtain for the shear angle:

$$\phi = \frac{\pi}{4} - \beta + \alpha \tag{13}$$

It further follows that the shear stress (τ) and the normal stress (σ) on this shear plane are equal. This conclusion disagrees with experimental evidence, and Lee postulated that this is due to the presence of the built-up edge. Figure 4 shows the analysis taking the built up edge into consideration. Again, using our notation, he obtained a modified expression for the shearing angle:

$$\phi = 45 + \psi - \beta + \alpha \tag{14}$$

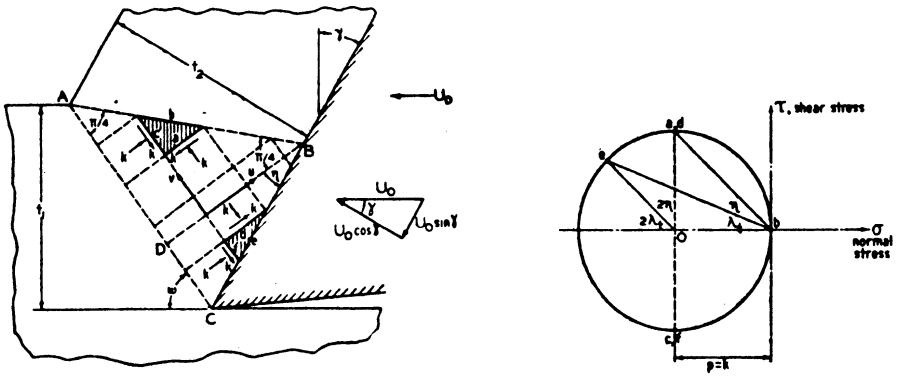

(a) Slip Line Field (b) Mohr Circle Diagram

Figure 3. Ideal Plastic Solution for Tool Point Stress Field in the Absence of a Built-Up Edge (Lee and Shaffer 54).

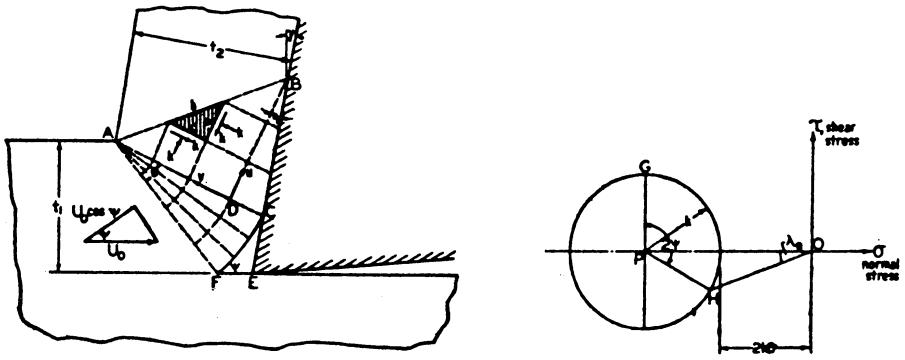

(a) Slip Line Field (b) Mohn Circle Diagram

Figure 4. Ideal Plastic Solution for Tool Point Stress Field in the Presence of a Built-Up Edge (Lee and Shaffer 54).

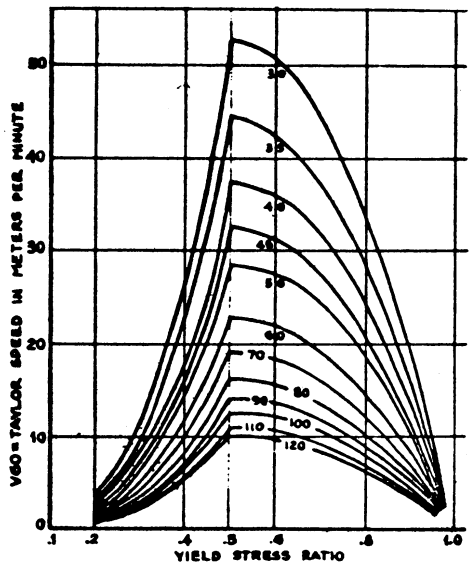

Figure 5. Relationship Between V_{60} and Mechanical Properties. (Janitzky 72).

where ψ is a measure of the size of the built up edge. Physically $\psi > 0$, and it follows from Mohr's circle that $\sigma > \tau$. Lee returned further to study the chip formation mechanism in his paper "The Theory of Discontinuous Machining."(55)

In 1952 Hucks(56,57) published the results of an extensive investigation of shear angle relationship. It led to a relation which is basically not different from the others. In 1953 Shaw(58) et al. studied the various aspects of the relation between friction and the shear angle in metal cutting, and a year later they published their paper on "Discontinuous Chip Formation."(59)

Hill(60) in 1954 explored the possible range of inclinations of the shear plane, by "excluding configurations that imply overstressing of material at the singularities of stress."

Okushima and Hitomi(61,62), in their very fine 1957 and 1958 papers investigated, both analytically and experimentally, the orthogonal cutting mechanism, by studying the transitional deformation range, the "flow region."

In 1959 Lamm(63) presented his "Hydrodynamic Theory" of chip formation, essentially descriptive and following his 1940 publication in the Soviet Union.(64)

Colding(65) in 1960 attempted with limited success to consider the unisotropy in the development of the shear angle.

Among the contributors to the theory of chip formation that were not discussed here for physical limitations are: Bastien, Kurrein, Leyensetter, Loladze(66), Opitz, Thomson, Weisz, Wallichs, Zorev(67) and others.

Machinability and Physical Properties

Since the extensive work by F. W. Taylor[7], practically every metal cutting researcher has devoted some of his time to study various aspects of machinability. The amount of work involved in evaluating machinability experimentally is very often objectionable. Millions of dollars have been spent by the United States Air Force in the early 1950's to evaluate the machinability of titanium and other alloys. Researchers recognized that the long tool life wear tests have to be replaced, either by shorter tests, or by an analytical method to predict machinability on the basis of the physical properties of the material.

Among the many tests that were suggested during these past fifty years to lower the testing time and expense, three deserve some attention. The first is the "constant pressure lathe" test, the second is the radioactive testing; and the third is the measurement of tangential cutting forces as a means to evaluate machinability.

By using the "constant pressure lathe" an attempt was made to "evaluate the materials on the basis of the feed resulting from fixed horizontal tool pressure."[68] Merchant[69], among others, in 1953 tried to use radioactive means to measure what he called an "instanteous rate of tool wear." His technique consisted of using tools "rendered radioactive by neutron irradiation in a nuclear reactor, collecting the resulting chips, and measuring their radioactivity due to the particles abraded from the tool during a few seconds of cut." This method in essence attempts to take the results of a very short time wear test and project the results on the long time wear process of the tool.

Schlesinger[70] was among those who believed that the tangential component of cutting force is a good criterion of machinability. He claimed further that the method actually compensates for the difference in the abrasiveness of the various materials. Unfortunately none of these methods was adequate for an arbitrary chosen material and short time machinability tests are still lacking.

The ability to predict machinability from physical properties has always been challenging. Janitzky[71], in 1938, related the machinability of steels to their Brinell Hardness (H_B) and their area reduction (A_r), as obtained in a standard tensile test. He expressed the functional relationship between the cutting velocity for a sixty minute tool life (V_{60}) and those variables as:

$$V_{60} = \frac{C}{H_B^{1.63} A_r^{1.01}} \tag{15}$$

Where C is a constant depending on the cutting conditions. Janitzky further claimed that "variation in chemical composition does not influence machinability provided that the steels may be heat treated to have the same mechanical properties."

In 1944 Janitzky[72] took a new look at the same problem. This time he correlated machinability with the tensile strength (σ_T) and the ratio of the yield strength (σ_y) to the tensile strength (σ_y/σ_T). The relationship obtained is given by Equations (16) and (17):

$$V_{60} = \frac{2C_1}{\sigma_T^{1.2}} \left(\frac{\sigma_y}{\sigma_T}\right)^2 \text{ for } \frac{\sigma_y}{\sigma_T} \leqslant 0.5 \tag{16}$$

$$V_{60} = \frac{C_1}{\sigma_T^{1.2}} \left[0.25 - \left(\frac{\sigma_y}{\sigma_T} - 0.5\right)^2\right] \text{ for } \frac{\sigma_y}{\sigma_T} \geqslant 0.5 \tag{17}$$

where C_1 is a constant depending on the cutting conditions. Figure 5 is a graphical representation of these two expressions for one set of cutting conditions.[73]

Unfortunately the mechanical properties are not the only physical properties affecting machinability, and therefore no generally valid solution should have been expected from Janitzky's studies. As to the hardness, it should be mentioned that Boston and Colwell[74] and Schlesinger[75] were among those to state that hardness alone is by no means a measure of machinability.

As a great part of the metal cutting research was devoted primarily to machinability of steels, attempts were made to correlate machinability with composition and with microstructure. The SAE Technical Report[76] on the effect of composition on machinability, and the United States Air Force Machinability Report No. 2[77] on the effect of microstructure on machinability seem to be the summary of the most extensive work in the respective areas.

It is evident that further study of the effect of physical properties on machiniability is necessary. This study is intended to fulfill part of that necessity.

III. EXPERIMENTAL PROCEDURES AND RESULTS

In this section the testing procedures used to determine the physical properties of the material are described first followed by those procedures used to evaluate their machinability.

Materials

The materials used in this investigation are steel, aluminum and molybdenum; their composition is given in Table I. They were all used in their "as received conditions" which are as follows: steel, hot rolled; 1100 aluminum hot forged and annealed; 2024 aluminum hot forged and precipitation hardened; molybdenum, arc-cast and extruded. Test specimens were taken from different parts of the bar stock to verify the uniformity of the material according to the following pattern: discs for hardness traverses were cut from both ends as well as from the half length of each bar; tensile, impact and wear specimens were cut from near the half length of the bar and specimens were made from several radial locations.

Tensile Tests

Tensile properties and true stress strain relations were determined on a Southwark Emery 60,000 lbs. hydraulic tensile testing machine. Three specimens with reduced sections, as shown in Figure 6 were tested of each material. The reduction in cross section had no noticeable effect on the true stress strain relations, and was introduced to facilitate measurement of the instantaneous circumference of the cross section. The

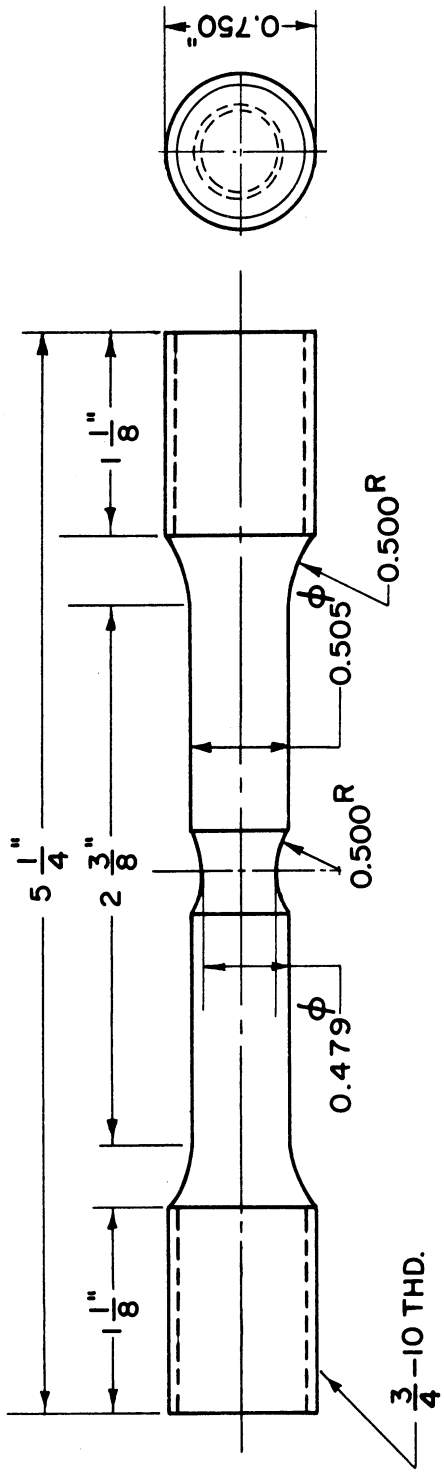

Figure 6. Tensile Specimen.

TABLE I

CHEMICAL ANALYSIS OF THE MATERIALS

	Material	C	Mn	P	S	Si	Ni	Cr	Mo	Fe	Cu	Mg	Ti	Zn	Al
1	AISI 1020	0.19	0.50	0.022	0.026	0.170	--	--	--	Bal	--	--	--	--	--
2	AISI 1212	0.06	0.89	0.100	0.200	0.006	--	--	--	Bal	--	--	--	--	--
3	AISI 1045	0.48	0.75	0.015	0.038	--	--	--	--	Bal	--	--	--	--	--
4	AISI 4340	0.41	0.74	0.011	0.020	0.350	1.77	0.80	0.27	Bal	--	--	--	--	--
5	Al 1100-0	--	0.01	--	--	0.09	--	--	--	0.56	0.13	0.01	0.01	--	Bal
6	Al 2024-T4	--	0.62	--	--	0.10	--	0.01	--	0.27	4.70	1.50	--	0.12	Bal
7	Molybdenum	0.028	--	--	--	--	--	--	Bal	--	--	--	--	--	--

area was computed from the circumference of the cross section, measured with a wire attached to a dial indicator.

A relationship of the form $\sigma = \sigma_0 \epsilon^m$ was found to be valid in the plastic region as shown in Figures 7 and 8, where σ is the true stress in psi, ϵ the true strain, and σ_0 and m are material constants, values of which are tabulated in Table II. The stress strain relations, corrected after necking began according to Bridgman[78] are given in Figures 7 and 8. Yield strength (σ_y) at 0.2% offset, tensile strength (σ_T), fracture stress (σ_{max}), fracture strain (ϵ_{max}) and reduction in area (A_r) were determined and are tabulated in Table III.

The flow stress (σ_F) was determined as the intersection of the plastic stress relation, $\sigma = \sigma_0 \epsilon^m$, with the elastic stress strain relation $\sigma = \epsilon E$, where E is Young's Modulus. This yields for the flow stress the value of $\sigma_F = \left[\frac{E^m}{\sigma_0}\right]^{\frac{1}{m-1}}$

Deformation energy (W) was computed to first approximation as:

$$W = \int_0^{\epsilon_{max}} \sigma \, d\epsilon = \sigma_0 \int_0^{\epsilon_{max}} \epsilon^m \, d\epsilon = \frac{\sigma_0 \epsilon_{max}^{m+1}}{m+1} \quad \left(\frac{lb\text{-}in}{in^3}\right) \qquad (18)$$

The values of W and σ_F are given in Table II.

Because of flaws in the molybdenum specimens they had to be tested in compression, and the data was modified to be compatible with the results of the tensile tests.

Hardness Tests and Meyer Strain Hardening Index

Several different hardness tests were conducted because no one scale is commonly used for the large range of hardness values of the materials under consideration.

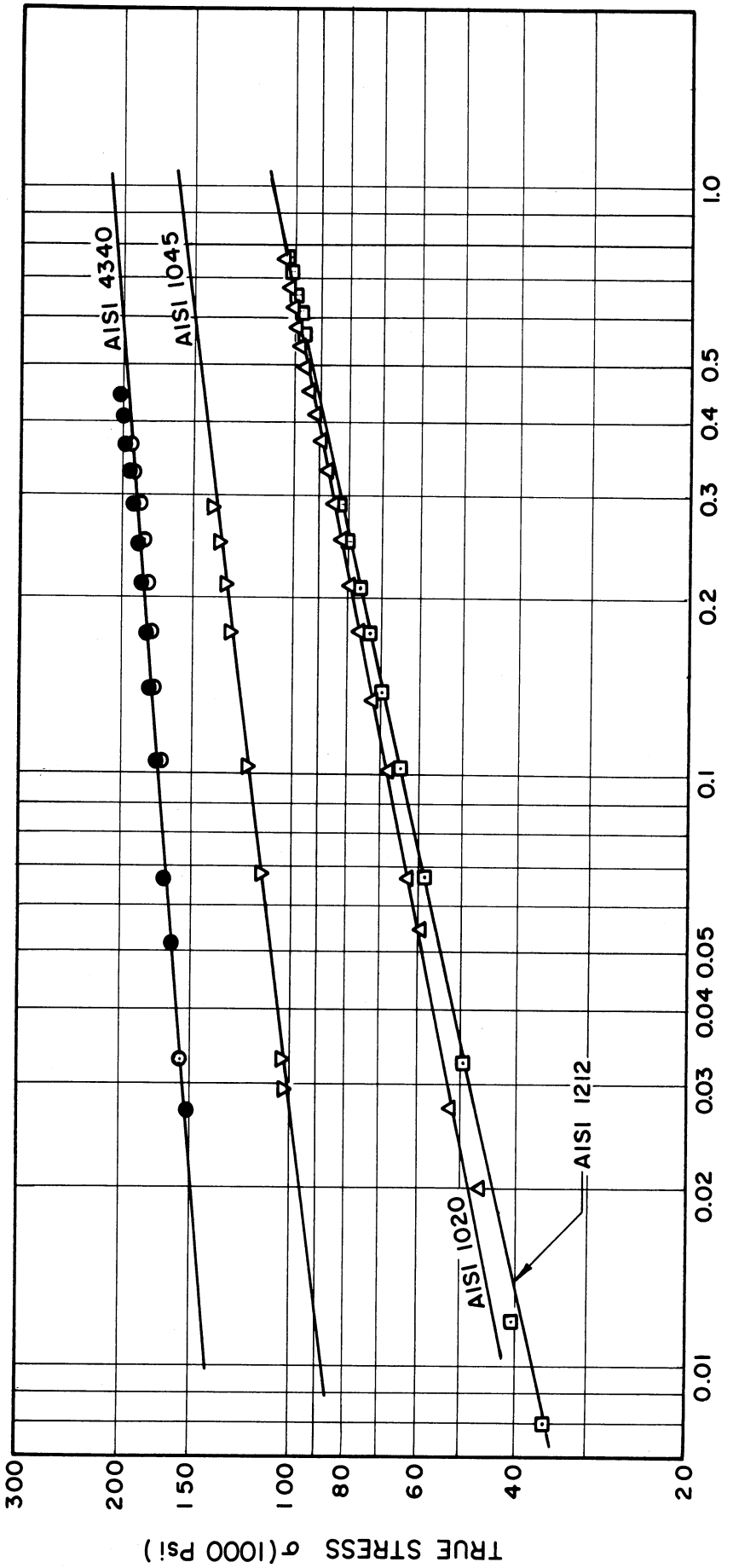

Figure 7. True Stress Strain Curves for Steels.

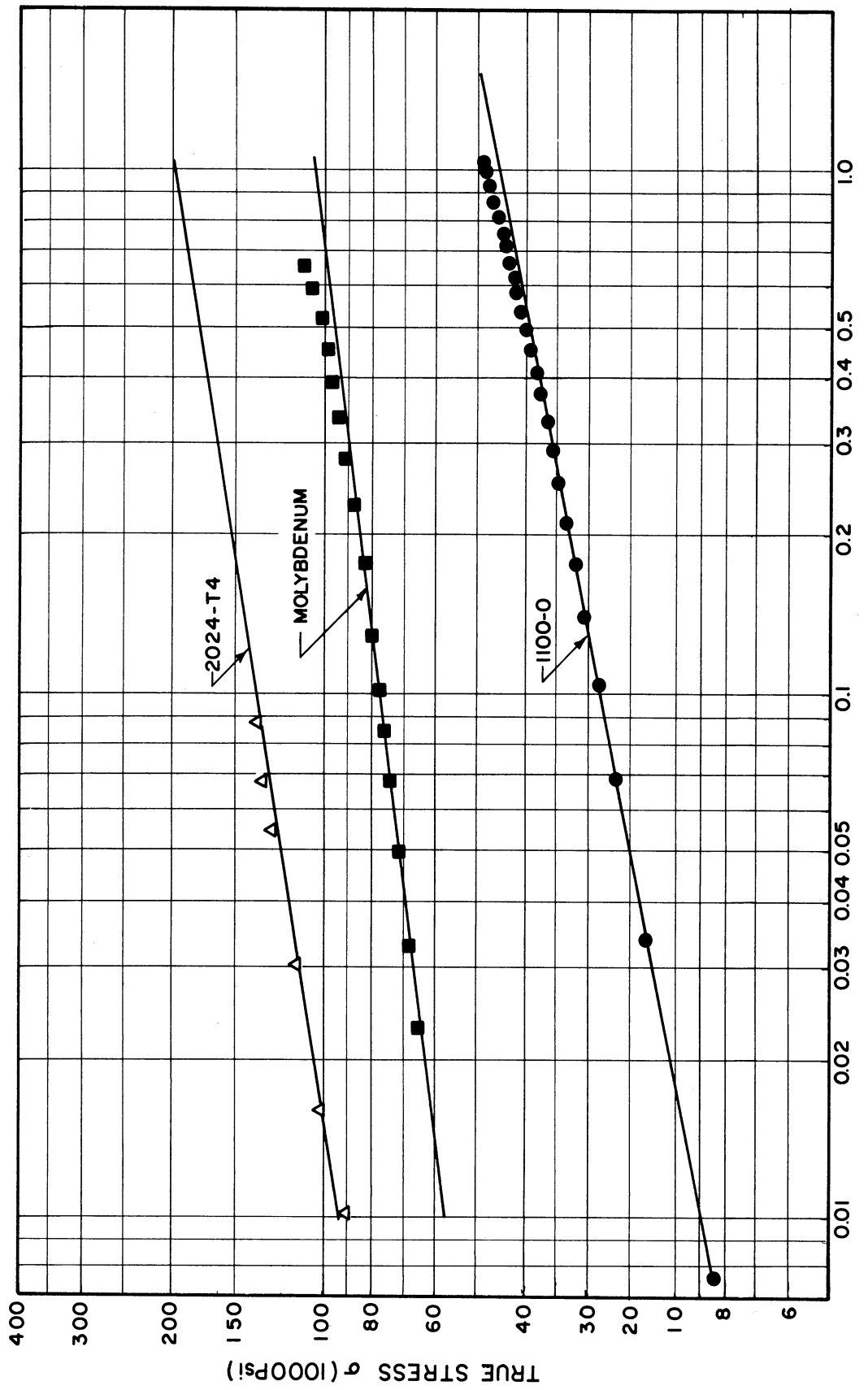

Figure 8. True Stress Strain Curves for Aluminum and Molybdenum.

TABLE II

STRESS STRAIN RELATION CONSTANTS,
FLOW STRESS AND DEFORMATION ENERGY

Material		Material Constants[1]		Flow Stress[2]	Deformation Energy[3]
		σ_o	m	σ_F	E
		psi	-	psi	in-lbs/in^3
1.	AISI 1020	110,000	0.211	24,500	75,600
2.	AISI 1212	110,000	0.235	20,000	73,800
3.	AISI 1045	160,000	0.134	72,000	47,000
4.	AISI 4340	210,000	0.088	118,000	80,700
5.	Al 1100-0	22,900	0.203	5,000	27,800
6.	Al 2024-T4	100,000	0.165	39,000	8,300
7.	Molybdenum	105,000	0.129	41,000	31,300

1. $\sigma = \sigma_o \epsilon^m$

2. $\sigma_F = \left(\frac{E^m}{\sigma_o}\right)^{\frac{1}{m-1}}$

3. $W = \int_0^{\epsilon_{max}} \sigma \, d\epsilon$

TABLE III

TENSILE PROPERTIES OF TEST SPECIMENS

Material	Yield Strength[1] σ_y psi	Tensile Strength σ_T psi	Fracture Stress σ_{max} psi	Fracture Strain ϵ_{max} -	Reduction in Area A_r %	Modulus of Elasticity E psi
1. AISI 1020	32,500	64,000	110,000	0.854	57.5	29×10^6
2. AISI 1212	28,000	61,000	105,000	0.855	57.5	29×10^6
3. AISI 1045	78,000	106,000	140,000	0.377	31.5	29×10^6
4. AISI 4340	135,000	153,000	195,000	0.446	36.0	29×10^6
5. Al 1100-0	6,900	13,500	28,000	1.342	74.0	10×10^6
6. Al 2024-T4	43,000	64,000	72,000	0.135	12.5	10.6×10^6
7. Molybdenum	49,500	80,500	91,000	0.388	32.0	54×10^6

[1]At 0.2% offset.

Rockwell and Brinell hardness tests were conducted on a Wilson Rockwell Hardness Tester and a Steel City Testing Laby Brinell Hardness Tester respectively.

The Brinell machine was also used to determine the Meyer hardness number and the Meyer[79] strain hardening index n. Meyer's law expresses the relation between the load and the size of the indentation of a spherical indenter. The equation is exponential and is expressed as $L = Kd^n$, where L is the load, d the chordal diameter of the remaining indentation, K and n are material constants. The latter is the Meyer index or the strain hardening exponent.

The average hardness values and Meyer's exponents are tabulated in Table IV. Meyer's relation is expressed graphically in Figures 9 and 10.

Impact Tests

A standard v-notch Charpy specimen, 0.394 x 0.394 x 2.165 inches was used for the impact tests. All notches were machined with the same new cutter.

A Sonntag Universal Charpy Impact Machine of 240 foot-pounds was used for the tests. Precautions were taken to ensure proper contact of the pendulum tup with the specimen surface opposite the notch. In each test, excluding the 1100-0 aluminum the anvil swung cleanly through the specimen without jamming the specimen in the machine. The aluminum 1100-0 specimens were bent but did not fracture.

Four specimens were tested of each material at a room temperature of 75°F, and the results are recorded in Table V.

TABLE IV

BRINELL, MEYER AND ROCKWELL HARDNESS NUMBERS
AND MEYER STRAIN HARDENING EXPONENT

	Material	Brinell Hardness Number		Meyer Hardness Number		Meyer Material Constants[1]		Rockwell Hardness	
		500 kg Load	3000 Kg Load	500 Kg Load	3000 Kg Load	K	n	B	C
		Kg/mm^2	Kg/mm^2	Kg/mm^2	Kg/mm^2	*	*	*	*
1.	AISI 1020	110	137	112	147	74.5	2.28	69.0	*
2.	AISI 1212	114	126	116	136	74.0	2.23	63.0	*
3.	AISI 1045	175	212	177	222	112.5	2.31	92.5	*
4.	AISI 4340	271	323	272	332	200.0	2.26	*	31.5
5.	Al 1100-0	28.4	*	30.0	*	14.9	2.24	*	*
6	Al 2024-T4	134	149	136	159	74.0	2.35	*	*
7	Molybdenum	175	195	177	205	109.0	2.28	87.5	*

[1]Constants in the relation $L = Kd^n$.

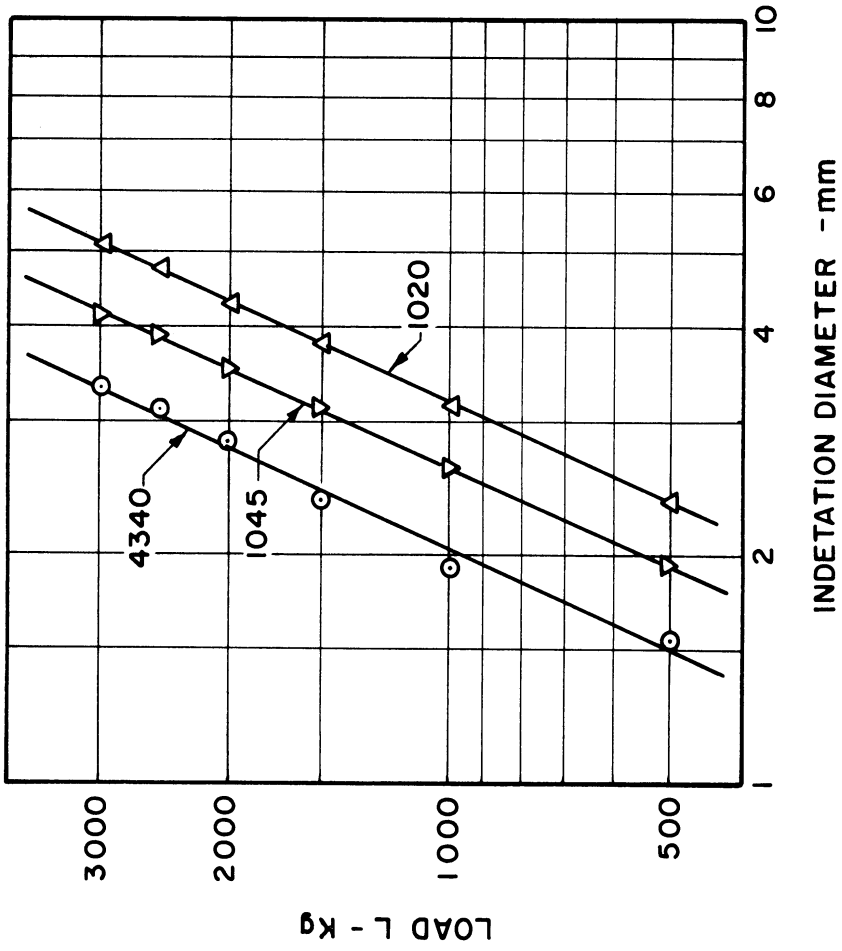

Figure 9. Meyer Relations for AISI 1020, 1045 and 4340 Steels.

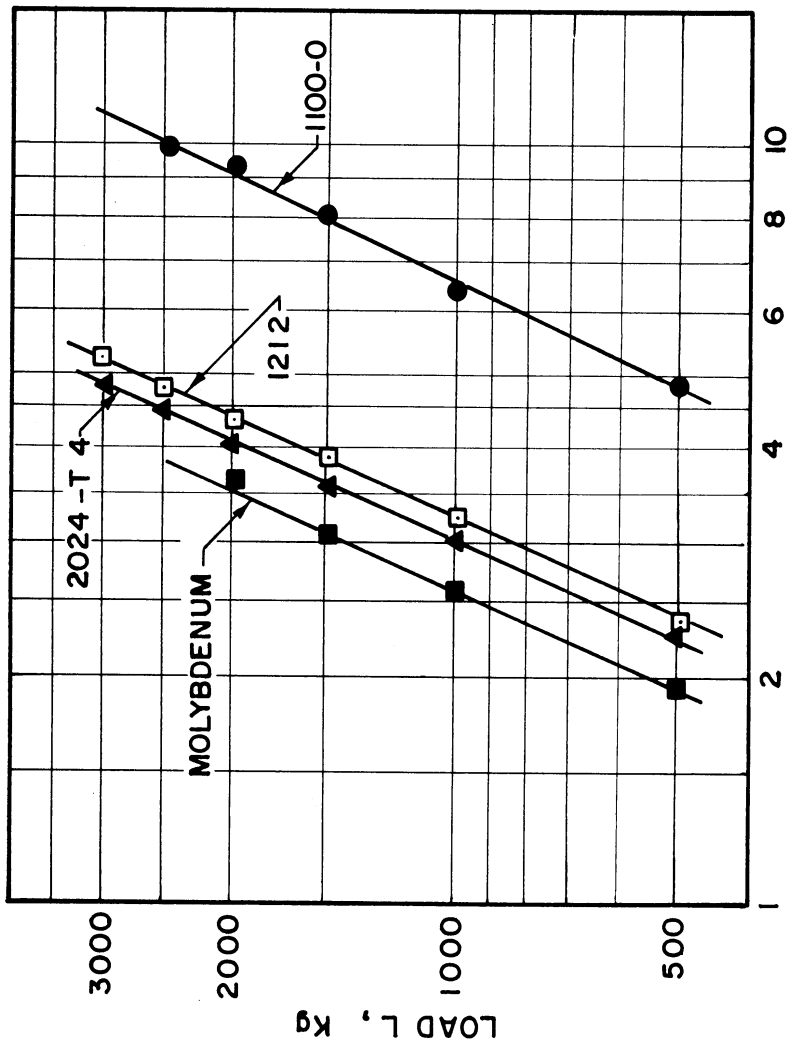

Figure 10. Meyer Relations for AISI 1212 Steel, Molybdenum, 1100-0 and 2024-T4 Aluminums.

TABLE V

CHARPY IMPACT STRENGTH OF TEST SPECIMENS

Material	IMPACT STRENGTH		
	Average Value	Minimum	Maximum
	Ft-lbs	Ft-lbs	Ft-lbs
1. AISI 1020	24.6	24.0	25.5
2. AISI 1212	8.9	8.0	9.8
3. AISI 1045	15.3	14.5	16.5
4. AISI 4340	5.6	4.0	7.5
5. Al 1100-0	54.9[1]	53.5	55.5
6. Al 2024-T4	5.1	5.0	5.2
7. Molybdenum	1.0	1.0	1.0

[1]Specimens did not break.

Thermal Properties

Thermal conductivity was determined by the "split block" comparative method, the standard for comparison being Armco Iron. Two measurements were conducted, below and above room temperature respectively, and room temperature values were obtained by interpolation. The tests were carried out at the Heat and Mass Transfer Laboratory, Armour Research Foundation of Illinous Institute of Technology.

Specific heat values were taken from the data compiled by Armour Research Foundation.

Density was determined by weighing cylindrical specimens of known dimensions on an analytical scale.

The above properties and the associated values computed from them are given in Table VI.

Metallography

A metallographic examination was conducted on all the materials under investigation.

The samples were mechanically polished through the 0, 00, and 000 dry papers. Final mechanical polish was performed on wet cloth with Linde A powder. The specimens were then etched and lightly repolished. The etching reagents used were Nital 2% for the steel, Keller's Reagent for the aluminum and 50% Nitric Acid for the molybdenum. The micrographs are given in Figures 11 to 17.

For the purpose of conducting a point count, a grid was superimposed photographically on the print of the microstructure.[80,81] This was achieved by exposing the printing paper first to the negative of the structure and then to the negative of the grid before developing it. Two

TABLE VI

THERMAL PROPERTIES OF TEST SPECIMENS AT 77°F

Material	Density	Specific Heat	Volume Specific Heat	Thermal Conductivity	Thermal Diffusivity
		C	ρC	K	α
	lb/ft^3	Btu/lb-°F	Btu/ft^3-°F	Btu/hr-ft-°F	Ft^2/hr
1. AISI 1020	488.3	0.120	58.6	30.3	0.52
2. AISI 1212	486.4	0.120	58.4	34.5	0.59
3. AISI 1045	487.4	0.120	58.5	25.1	0.43
4. AISI 4340	488.3	0.120	58.6	19.3	0.33
5. Al 1100-0	168.6	0.230	38.8	121.0	3.12
6. Al 2024-T4	173.7	0.230	40.0	71.2	1.78
7. Molybdenum	637.7	0.065	42.1	69.6	1.65

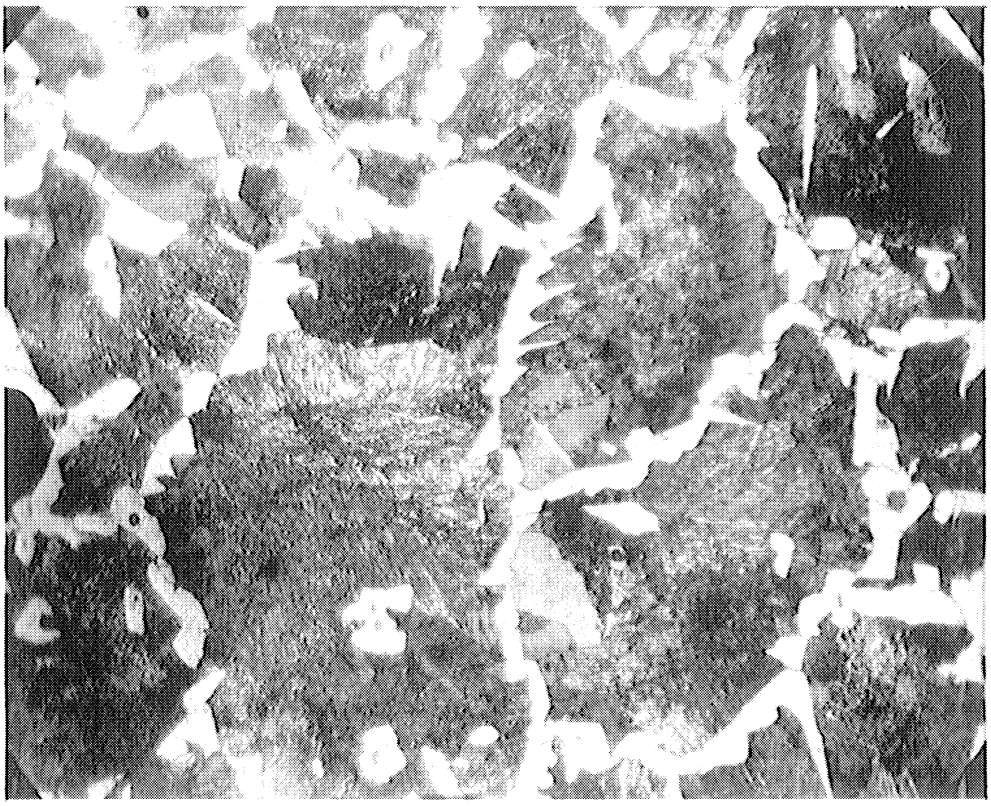

Figure 11. AISI 1045 Steel, Hot Rolled (500 X, Nital Etch).

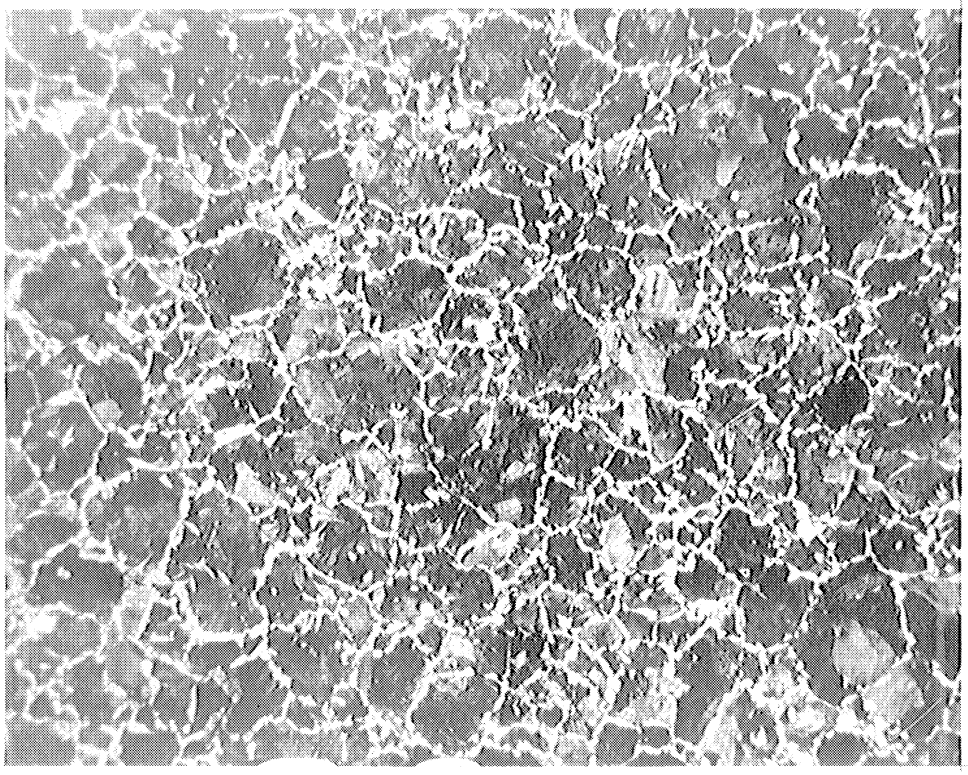

Figure 12. AISI 1045 Steel, Hot Rolled (100 X, Nital Etch).

Figure 13. AISI 4340 Steel, Hot Rolled (100 X, Nital Etch).

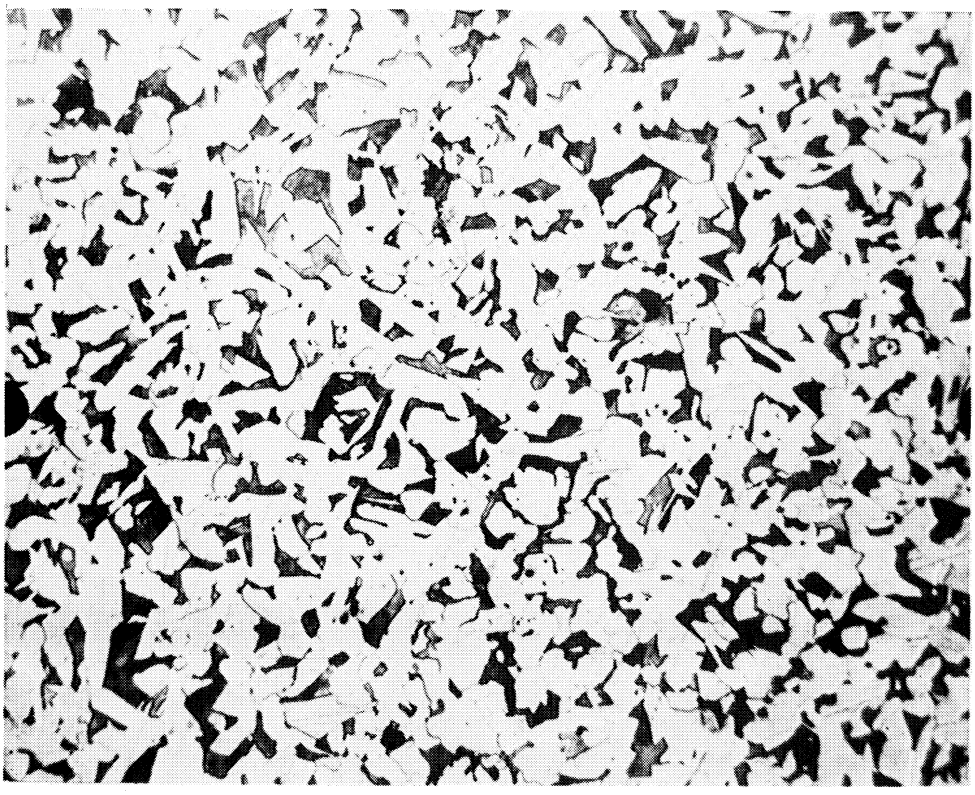

Figure 14. AISI 1020 Steel, Hot Rolled (100 X, Nital Etch).

Figure 15. 2024-T4 Aluminum, Solution Heat Treated (100 X, Keller's Etch).

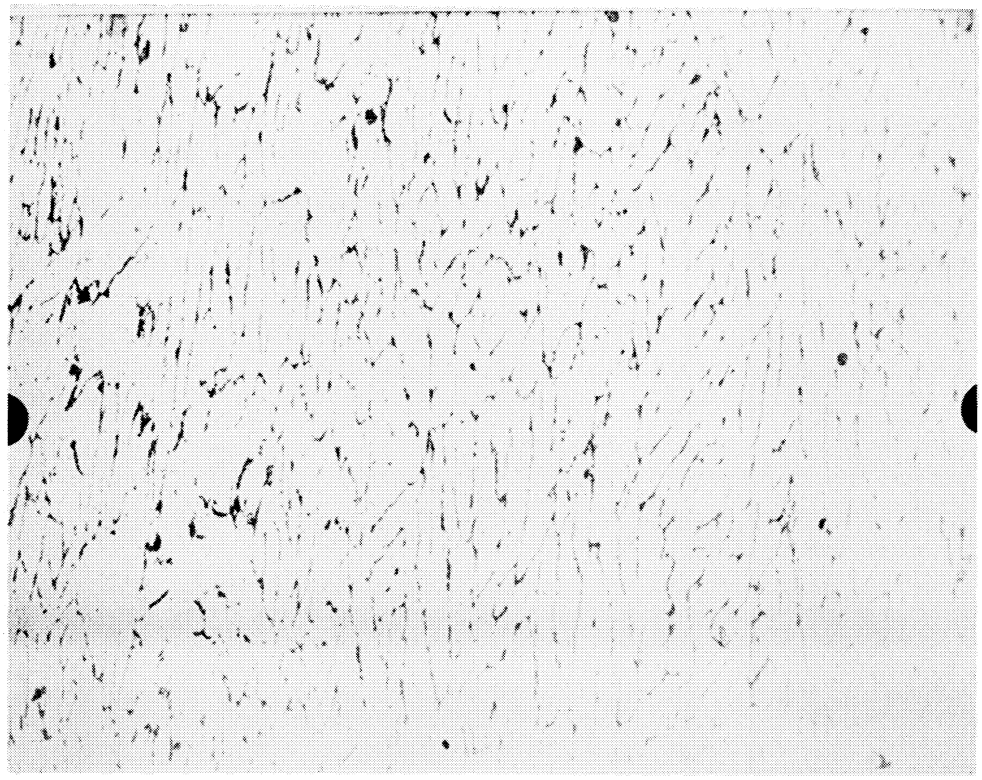

Figure 16. 1100-0 Aluminum (100 X, Keller's Etch).

Figure 17. Molybdenum, Arc Cast and Extruded (100 X, 50% HNO_3 Etch).

examples are shown in Figures 18 and 19 and the results are tabulated in Table VII.

The percent of ferrite and pearlite in the microstructure was also computed on the basis of the chemical analysis.[82] The analysis and the comparison with the results of the point count are given in Table VII.

The analytical method is considered more reliable than the point counting for various reasons. First, it is less influenced by the subjective impressions of the investigator. Secondly, finely dispersed microconstituents require a high magnification for the point counting, resulting in a highly localized picture, which is in most instances not representative of the sample. And thirdly, the portion of the second phase being at the grain boundaries cannot be counted.

Microhardness Measurements of the Chip

As Herbert[91] has already suggested that the hardness of the chip could be a measure of machinability, it was considered appropiate to investigate this statement further. Cuts were conducted at various speeds, the chips were mounted, polished and etched, and Knoop microhardness measurements were taken. Figure 20 shows an AISI 1020 steel chip with the hardness reading superimposed on it. Similar microhardness tests were conducted on all the materials studied. It is seen clearly that the strain hardening of various grains is extremely different, and that in general, as expected, the softer phase, the ferrite, deformed more than the harder phase, the pearlite. It was impossible to draw any conclusions about the machinability of the work material, neither from

TABLE VII

PEARLITE CONTENT OF THE STEELS

MATERIAL	Carbon Content %	Carbon Content of Eutectoid %	PEARLITE Computed %	CONTENT Point Count %
1. 1020 AISI	0.19	0.750	25.3	21.5
2. 1212 AISI	0.06	0.755	7.9	3.6
3. 1045 AISI	0.48	0.735	65.3	74.4
4. 4340 AISI	0.41	0.425	96.5	100.0

1. $C = \frac{A}{B} \times 100$

the maximum, nor from the average hardness of the chips. The problem was further complicated on examining the effect of the depth of cut on chip hardness.

Hardness of the chip is by no means a property of the material, though it is obviously dependent on the material's properties. It would have been justified to use it, if it gave a clear cut quantitative indication of the machinability of the work material. It did not, and Herbert's statement is considered to be an oversimplification of the problem.

Machinability Tests

Single point tool life tests in which progressive wear was measured were conducted on all the experimental materials.

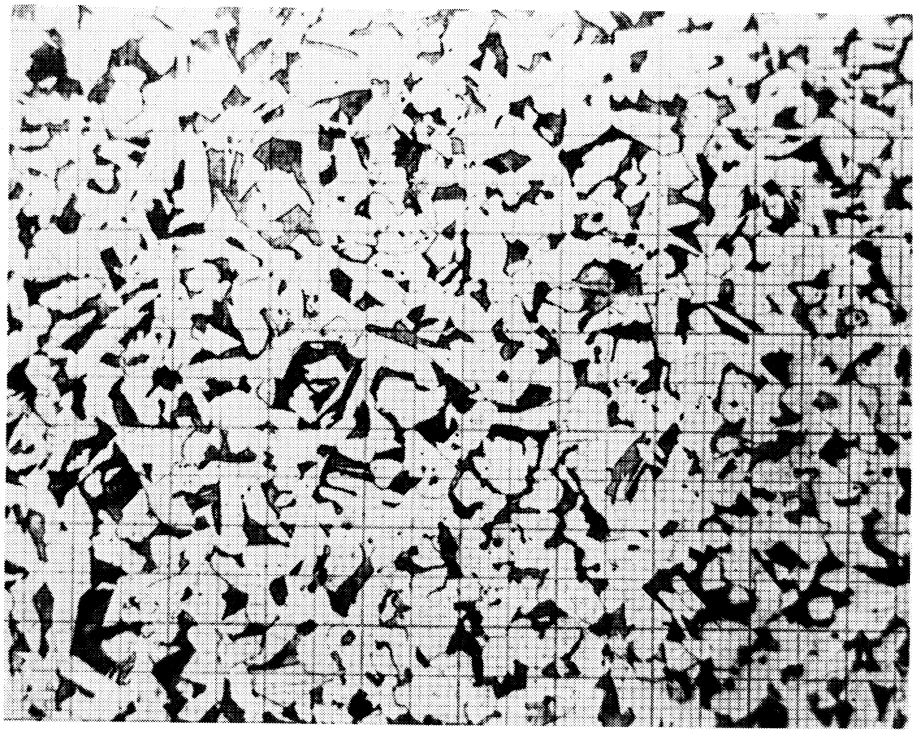

Figure 18. AISI 1020 Steel, Hot Rolled, Grid Superimposed for Point Count (100 X, Nital Etch).

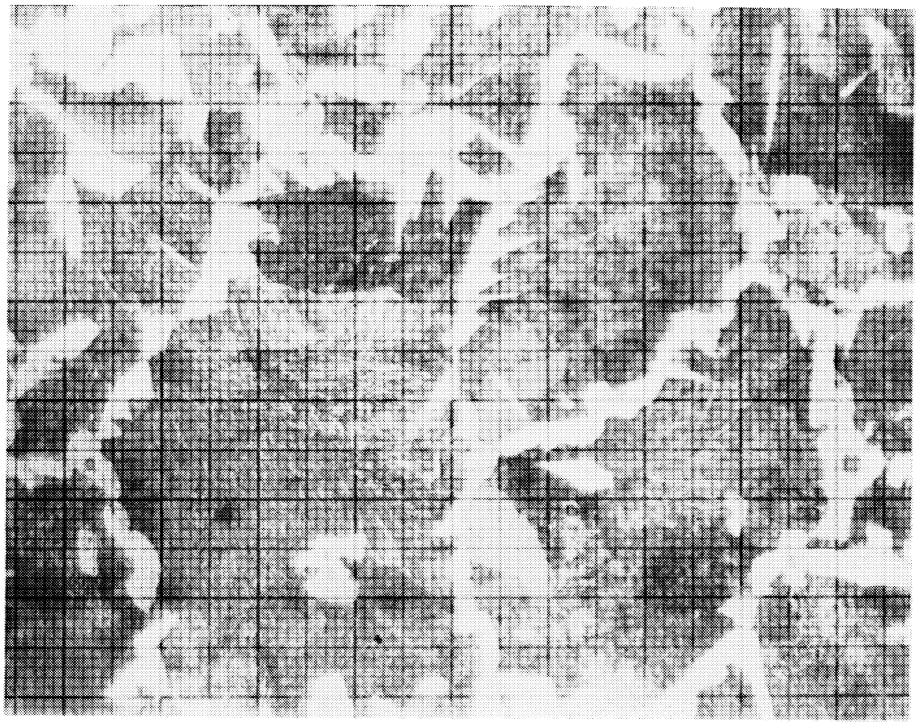

Figure 19. AISI 1045 Steel, Hot Rolled, Grid Superimposed for Point Count (100 X, Nital Etch).

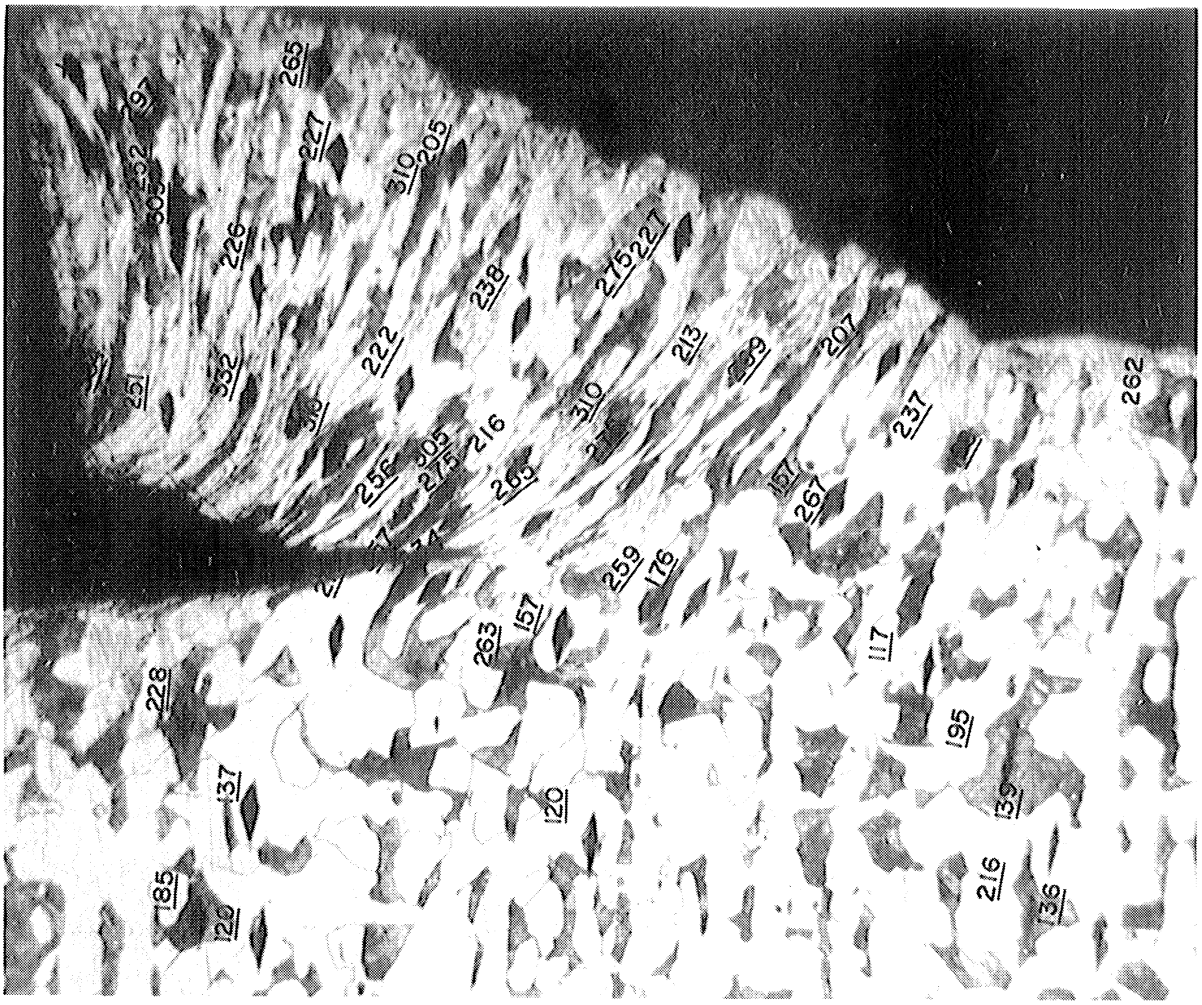

Figure 20. Knoop Microhardness Measurements on an AISI 1020 Steel. Cutting Velocity V = 0.020 in/min, Depth of Cut t = 0.010 in, Width of Cut w = 0.100 in, Rake Angle 10°.

Commonly used standard T-1 high speed steel tool material was selected in order to minimize the testing time and the material requirements.

As no one tool geometry is optimum for all the materials that could be encountered, the simplest geometry, ASA designation 0, 0, 7, 7, 7, 0, 0 was chosen. The details of the tool geometry and nomenclature are given in Figure 21.

The tools were ground on a Cincinnati Tool Grinder to a 12-15 RMS surface finish, all with the same 48A80-H5-V8 grinding wheel.

The machinability tests were conducted on a 14" swing American Pacemaker engine lathe with a variable speed drive.

Turning cuts, with a constant depth of 0.050 inch a constant feed of 0.0057 inch/revolution were carried out at various speeds. Cutting speeds were selected to give a tool life between one and one hundred and twenty minutes, preferably between 10 and 60 minutes. All tests were conducted dry.

In the first set of tests, the cuts were interrupted periodically to inspect the wear of the cutting edge. Flank wear, crater wear, and end wear, if present, were measured and recorded with the aid of a toolmaker's microscope. Figure 22 shows typical wear curves obtained for the different materials in this investigation. Machining time corresponding to a flank wear of 0.100 inch was defined as "tool life" for the purpose of this study, which is a standard procedure.

In the second set, the tests were conducted continuously to complete destruction of the cutting edge.

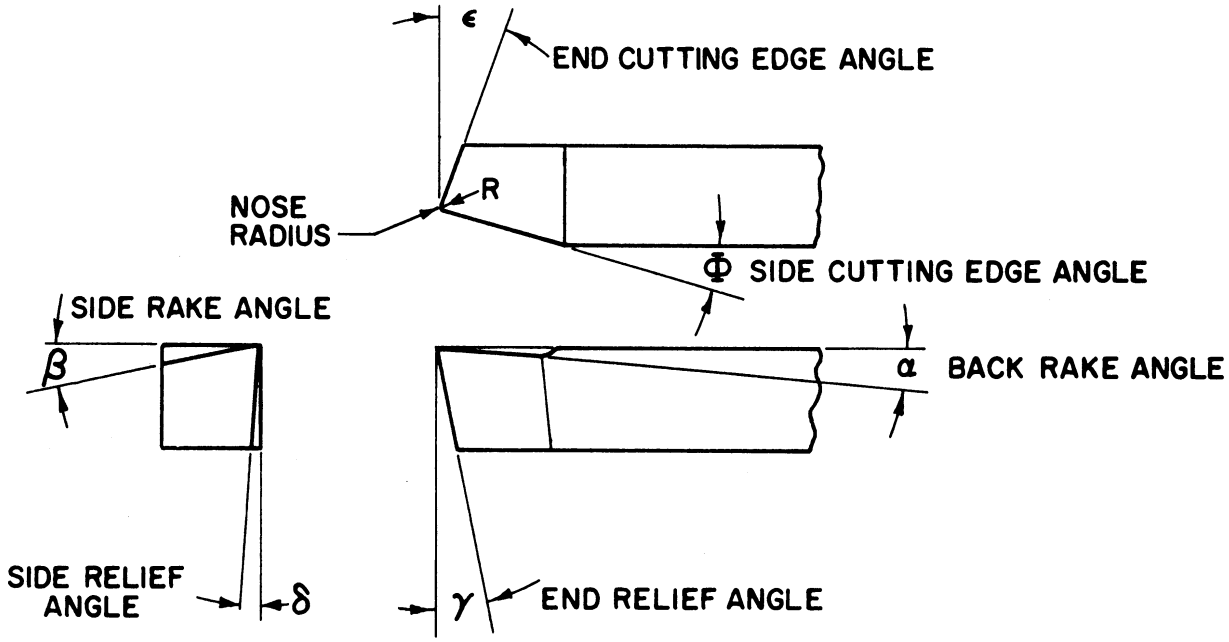

α	Back Rake Angle
β	Side Rake Angle
γ	End Relief Angle
δ	Side Relief Angle
ϵ	End Cutting Edge Angle
Φ	Side Cutting Edge Angle
	Nose Radius

Figure 21. ASA Single Point Tool Geometry and Designation.

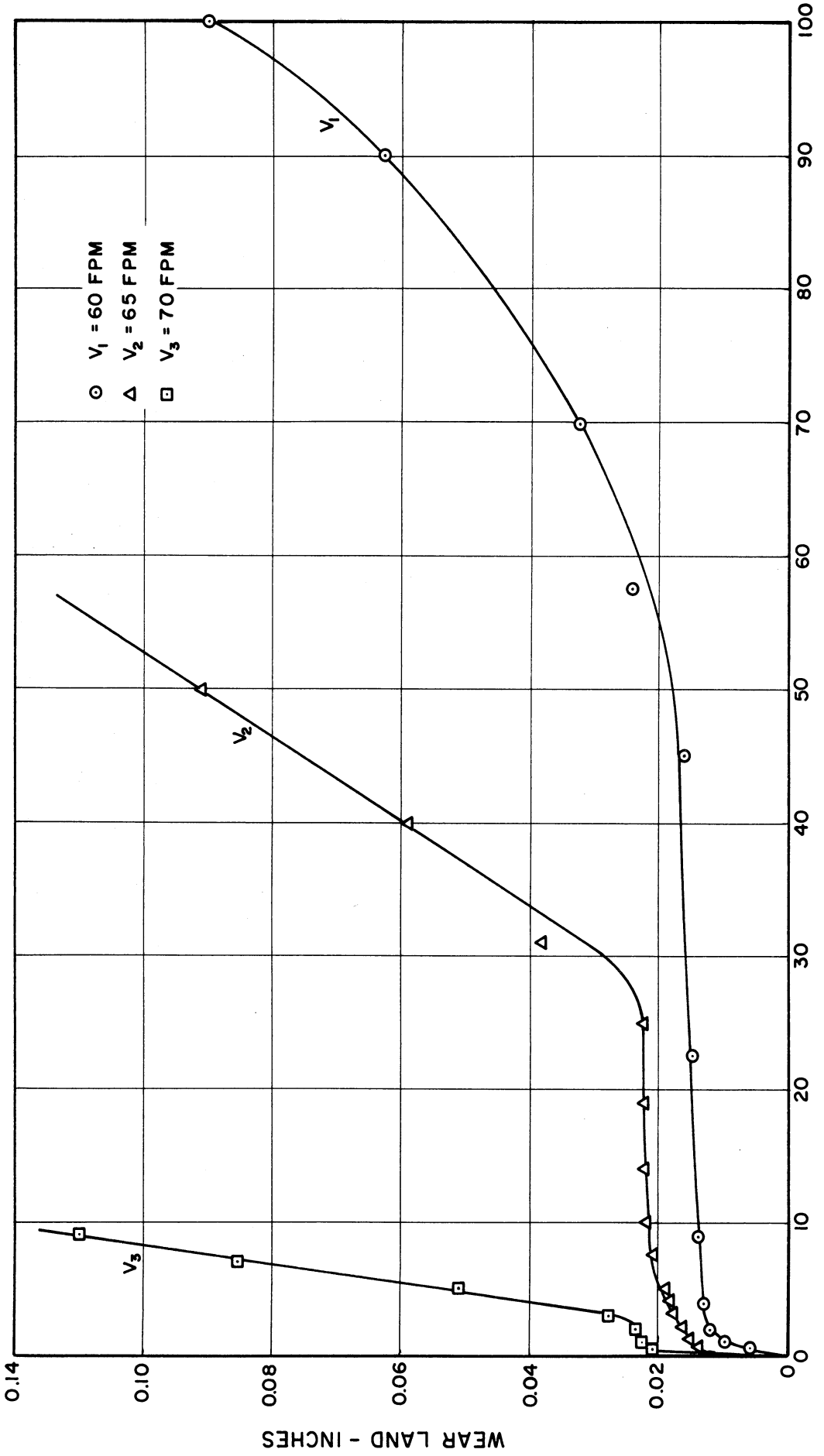

Figure 22. Typical Wear Curves. Material AISI 4340 Steel.

The tool life curves were found to agree with, for the common range of velocities shown in Table VIII, the Taylor relationship $VT_L^n = C$, where T_L is the tool life in minutes, V the cutting velocity in FPM, and C and n are constants depending on the cutting conditions and the materials machined. C is the cutting velocity that yields a one minute tool life, and n is the slope of the above plot in a log-log coordinate system.

The method of least squares, the general analysis of which follows, was applied to determine the tool life relationship from the experimental data. The following is the analysis carried out to evaluate the constants C and n in the tool life equation

$$VT_L^n = C \tag{19}$$

rewrittn in logarithmic form

$$\ln V = \ln C - n \ln T_L \tag{20}$$

$$\text{Set} \begin{cases} \ln V = y \\ \ln T_L = x \\ \ln C = a \\ -n = b \end{cases} \tag{21}$$

$$y = a + bx \tag{22}$$

Sum over all equations N:

$$\sum_1^N y = \sum_1^N a + b \sum_1^N x \tag{23}$$

Note that $\sum_1^N a = Na$

$$\therefore \sum_1^N y = Na + b \sum_1^N x \tag{24}$$

Multiply Equation (22) by x:

$$xy = ax + bx^2 \tag{25}$$

Sum all equations N:

$$\sum_{1}^{N} x\,y + a \sum_{1}^{N} x + b \sum_{1}^{N} x^2 \tag{26}$$

Solving Equations (24) and (26) for a and b will yield the following solutions:

$$a = \frac{\Sigma\, x \,\Sigma\, x\, y - \Sigma\, x^2 \Sigma\, y}{\Sigma\, x \,\Sigma\, x - N \,\Sigma\, x^2} \tag{27}$$

$$b = \frac{\Sigma\, x \,\Sigma\, y - N \,\Sigma\, xy}{\Sigma\, x \,\Sigma\, x - N \,\Sigma\, x^2} \tag{28}$$

where the summation is over all values N. Substituting back the values from Equation (21) gives the final answer for the two constants C and n:

$$\ln C = \frac{\Sigma\,(\ln V)\,\Sigma\,(\ln T_L)^2 - \Sigma\,(\ln T_L)\,\Sigma\,(\ln T_L)\,(\ln V)}{N\,\Sigma\,(\ln T_L)^2 - \Sigma\,(\ln T_L)\,\Sigma\,(\ln T_L)} \tag{29}$$

$$n = \frac{\Sigma\,(\ln V)\,\Sigma\,(\ln T_L) - N\,\Sigma\,(\ln V)(\ln T_L)}{N\,\Sigma\,(\ln T_L) - \Sigma\,(\ln T_L)\,\Sigma\,(\ln T_L)} \tag{30}$$

The values of the constants C and n, and the range of validity of the tool life equations are tabulated in Table VII and a sample computation is given in Appendix A. The results of the machinability tests are presented in Figures 23, 24, and 25.

The excellent machinability of 1100-0 aluminum prevented us from obtaining the actual tool life cutting velocity relationship. We could neither reach cutting velocities above 4400 fpm to measure tool chip

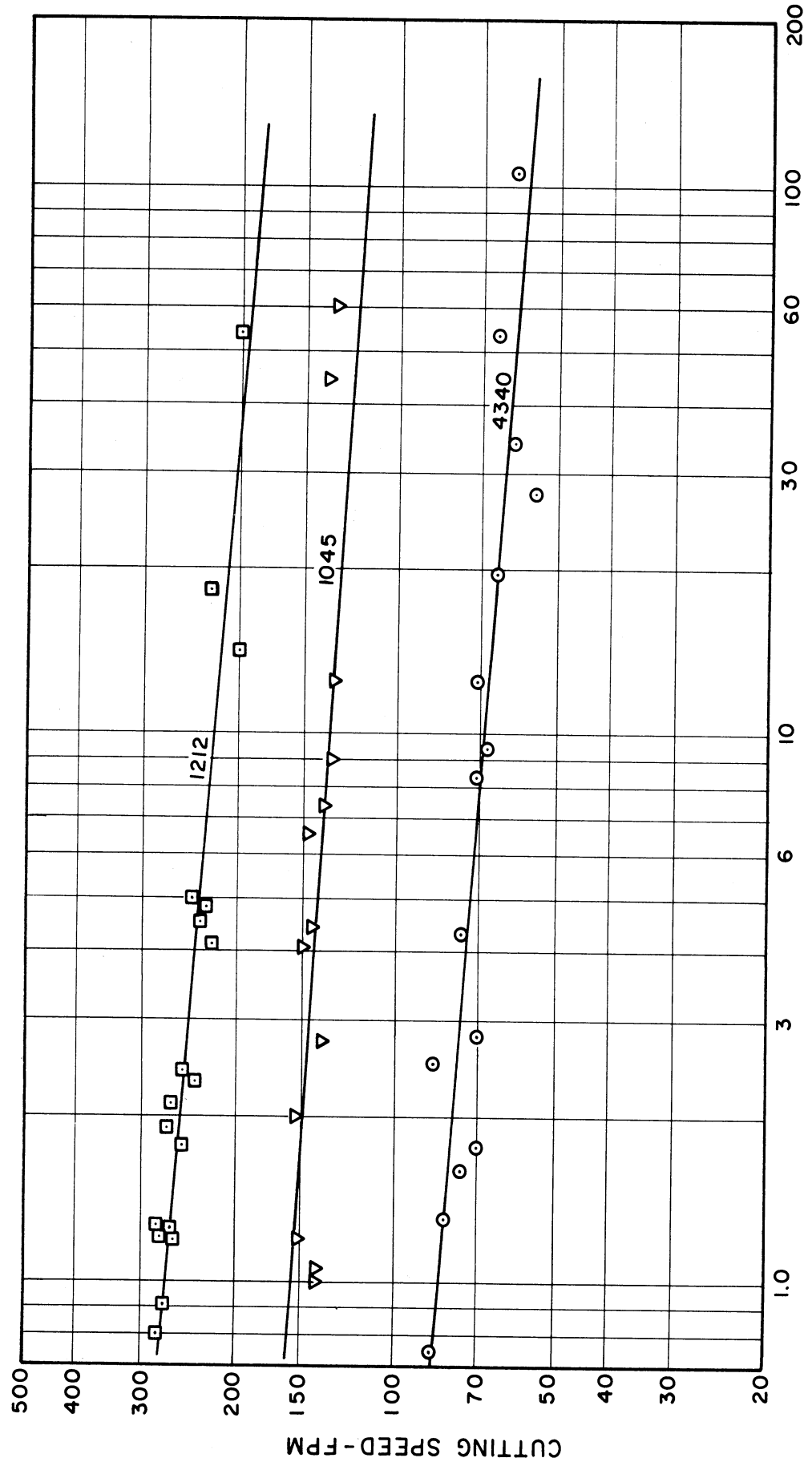

Figure 23. Cutting Speed - Tool Life. AISI 1212, 1045 and 4340.

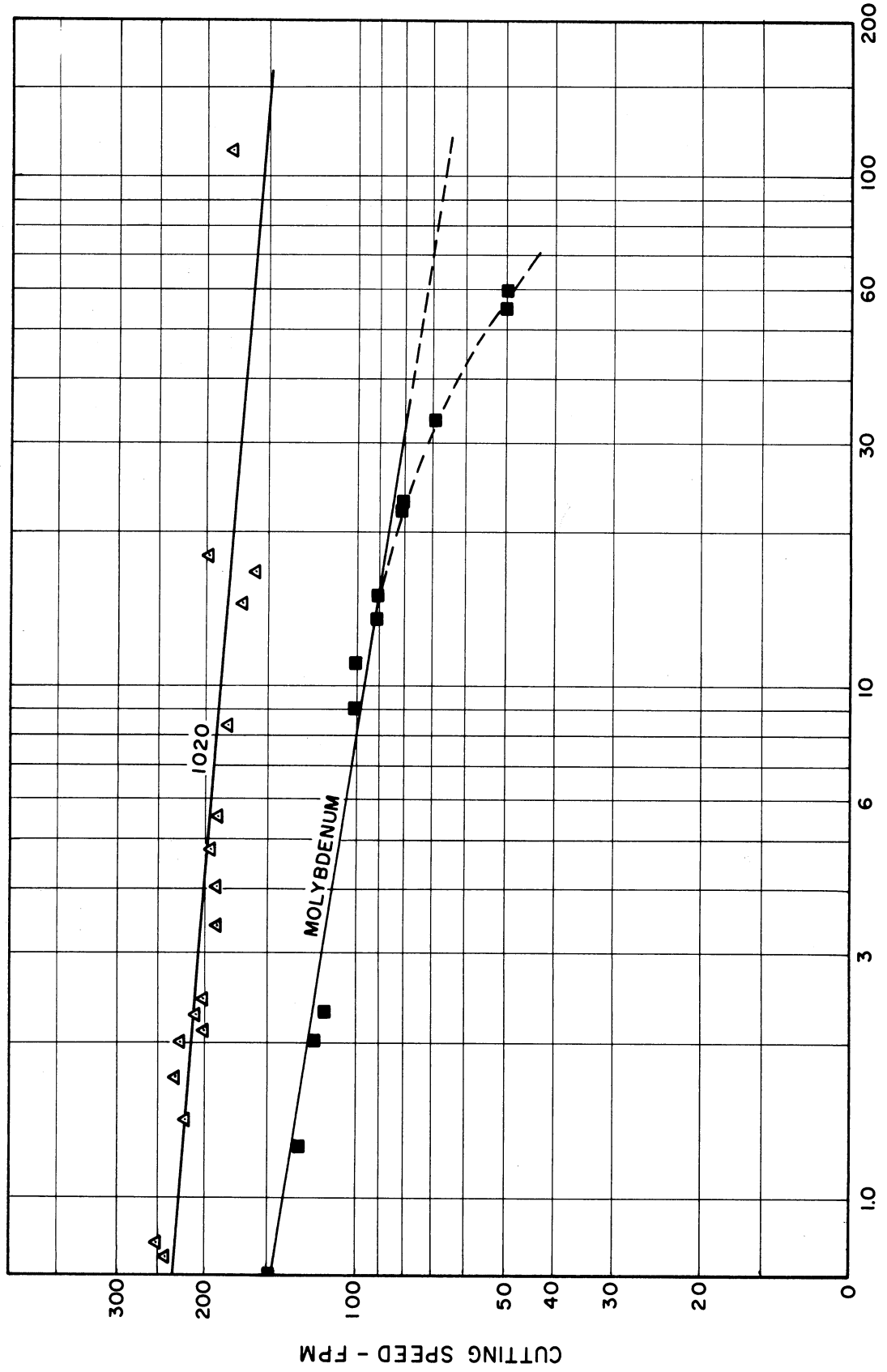

Figure 24. Cutting Speed - Tool Life. AISI 1020 and Molybdenum.

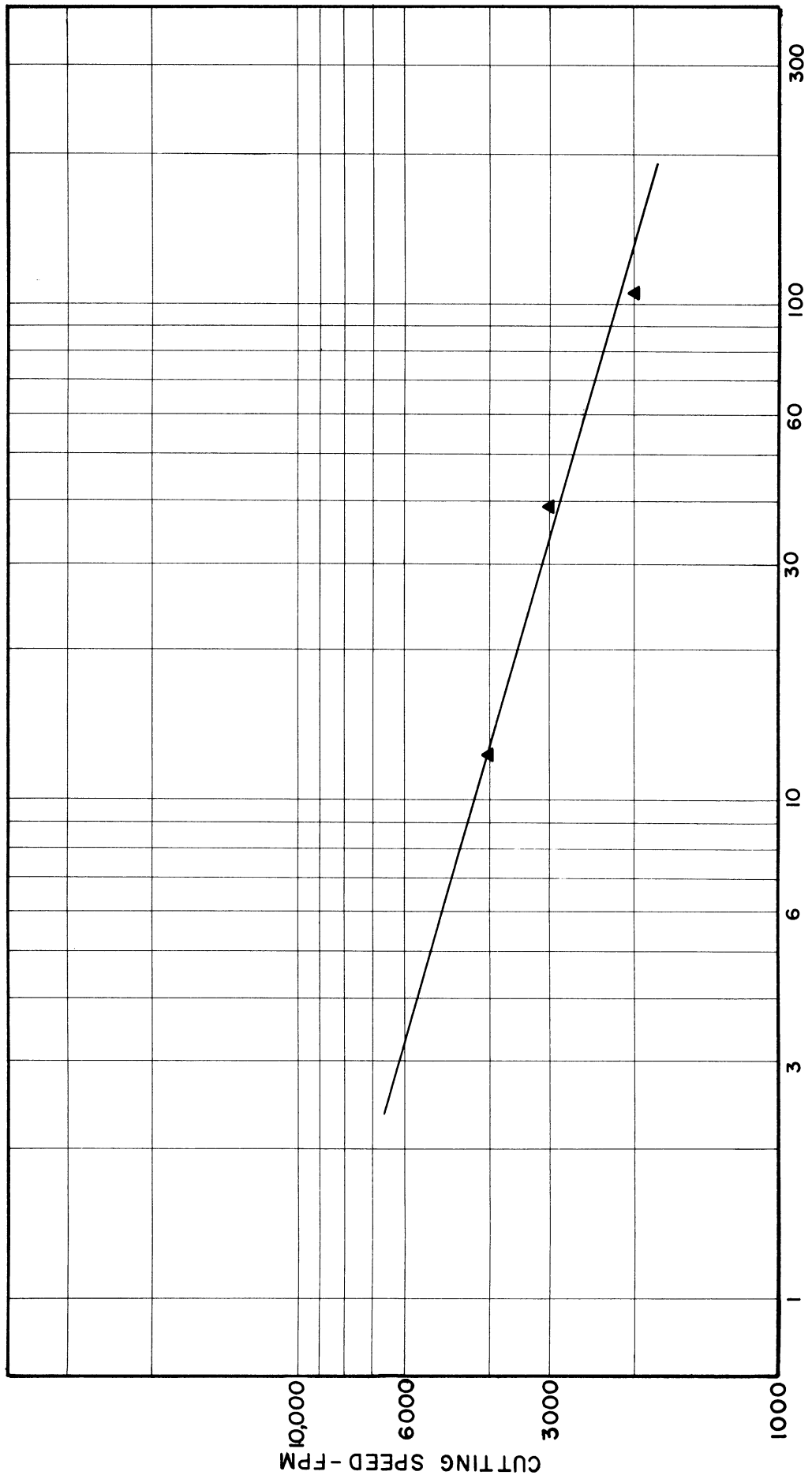

Figure 25. Cutting Speed Tool Life. 2024-T4 Aluminum.

interface temperatures, nor fail the tool because of material limitations. With a cutting speed of 4000 fpm the tool showed only 0.016 inches of flank wear after thirty minutes of cutting. Therefore we had to extrapolate the wear curves, and predict a cutting velocity of about 8500 fpm for a sixty minute tool life.

TABLE VIII

CUTTING SPEED - TOOL LIFE CONSTANTS

	Constants[1]		Cutting Speed Range of Validity	
Material	C	n	V_L^2	V_u^3
	-	-	FPM	FPM
AISA 1020	225	0.081	150	230
AISA 1212	270	0.085	180	270
AISA 1045	156	0.066	120	160
AISA 4340	82	0.078	55	85
Al 1100-O[4]	*	*	*	*
Al 2024-T4	8450	0.300	2000	4000
Molybdenum	137	0.158	90	140

1. $VT_L^n = C$
2. V_L - lower limit
3. V_u - upper limit
4. No Taylor relationship obtained.

Cutting Temperatures

Cutting temperatures, being indicative of the cutting process, were determined for all materials under investigation.

The tool chip interface temperatures were measured by using two tool-work thermocouples, described schematically in Figure 26. The method due to Gottwein and Reichel[33, 83] is, despite its limitations, an acceptable way to evaluate cutting temperatures. It is definitely the simplest, as it is independent of the work material, and therefore requires only one calibration for the set of tools used in the experiment.

For the purpose of this investigation, one tool was the high speed steel tool used in the machinability tests, and the other a cast non-ferrous, Crobalt No. 2. The temperature - EMF characteristics were determined by inserting the two tools into a metallic bath of known temperature, and measuring the generated EMF with a Sanborn Low Level Preamplifier. Precautions were taken to keep the cold junction at room temperature. The calibration curve is given in Figure 27.

The tools were then used to evaluate the cutting temperatures for the different materials under the same conditions that the machinability tests were conducted. A newly ground tool was used for each test.

The temperature velocity relationship was found to be of the exponential form $\theta = AV^a$, where θ is the tool chip interface temperature in °F, V the cutting velocity in FPM, and A and "a" are constants depending on the cutting condition and the material tested.

Table IX gives the values of the constants and the range of velocities within which the temperature velocity relationship is valid. The cutting temperature plots are given in Figures 28, 29, and 30.

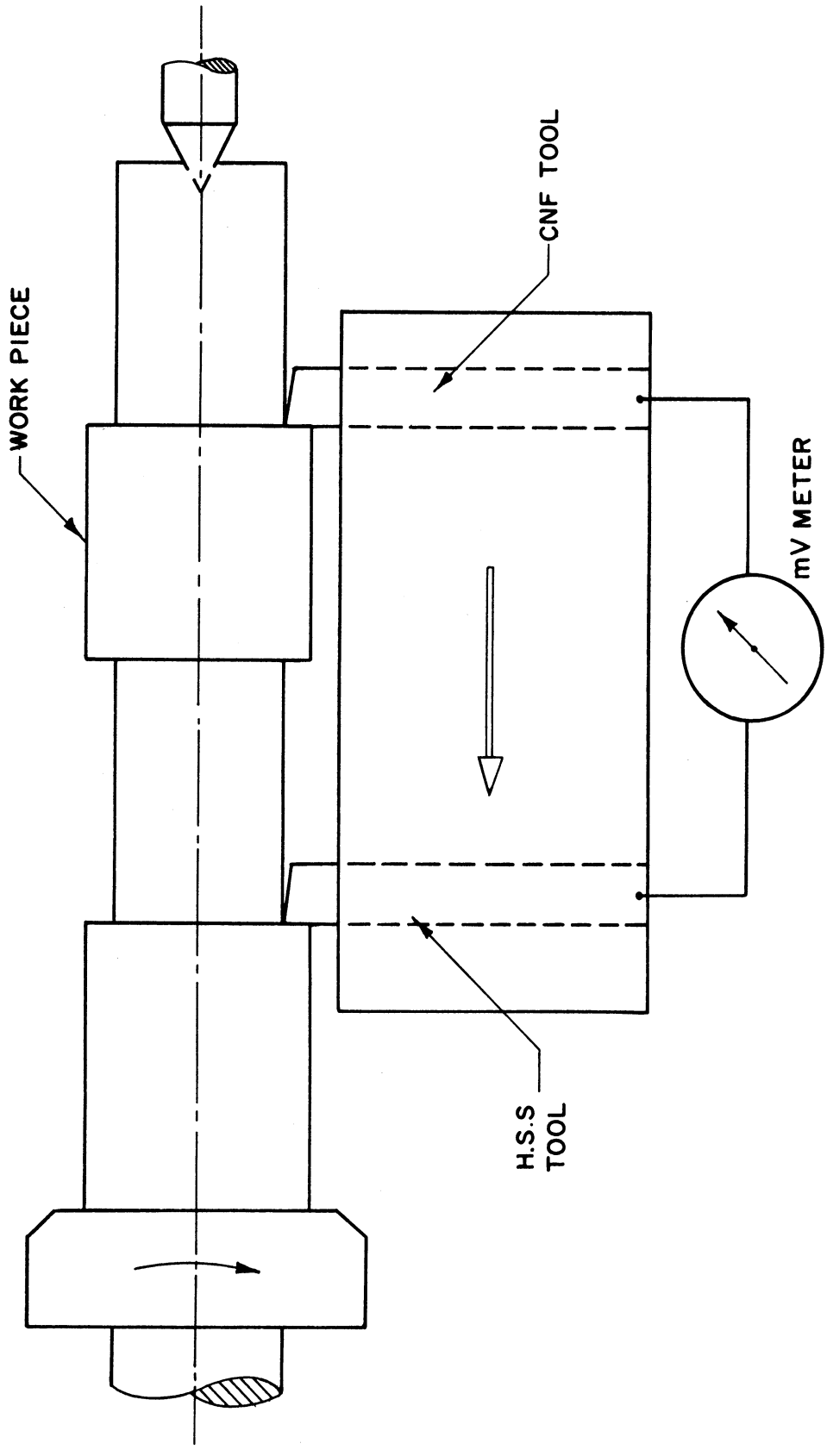

Figure 26. Duo Tool-Work Thermocouple for Measuring Cutting Temperature.

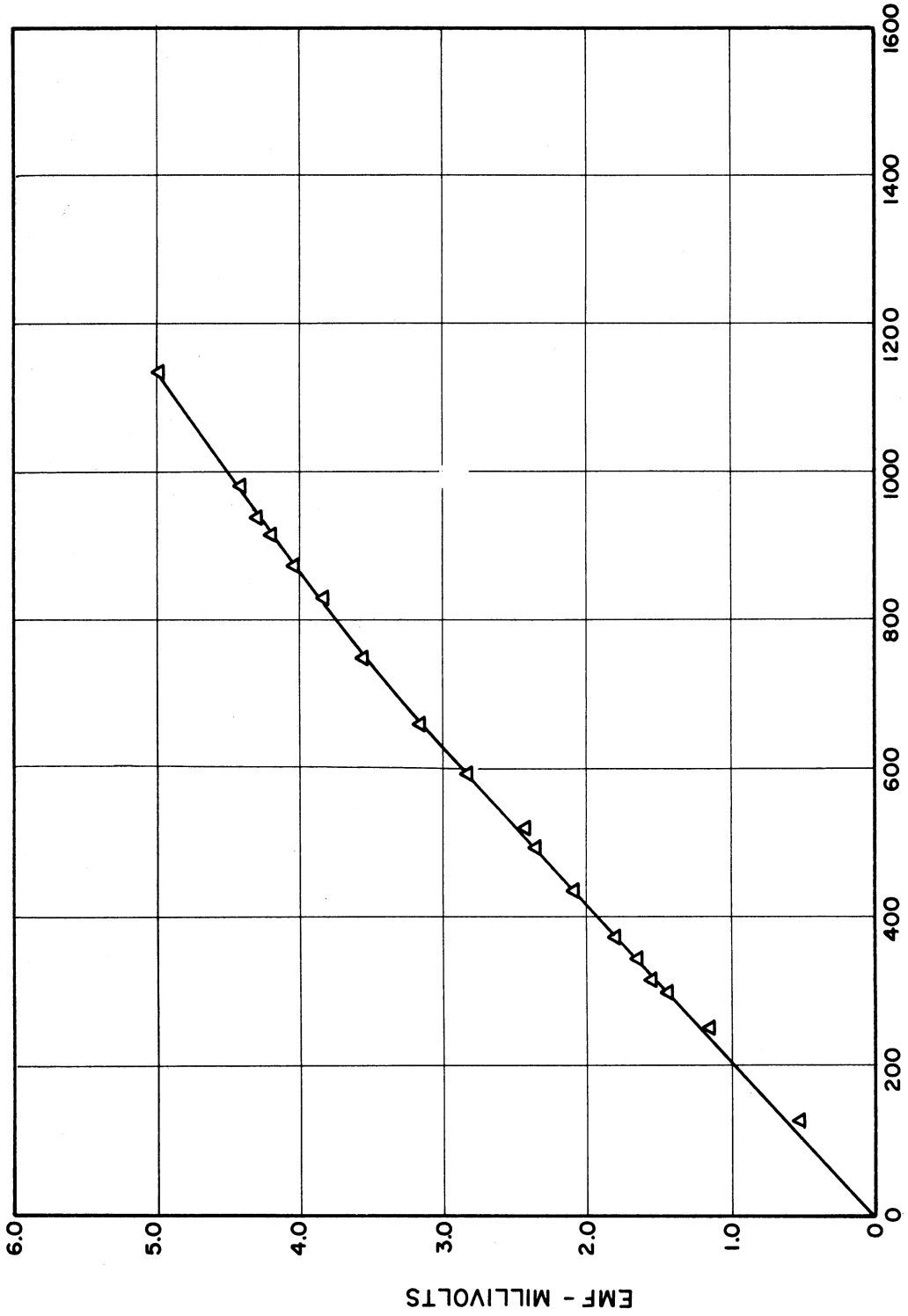

Figure 27. Temperature EME Characteristics of High Speed Steel vs. Cast Nonferrous Tools.

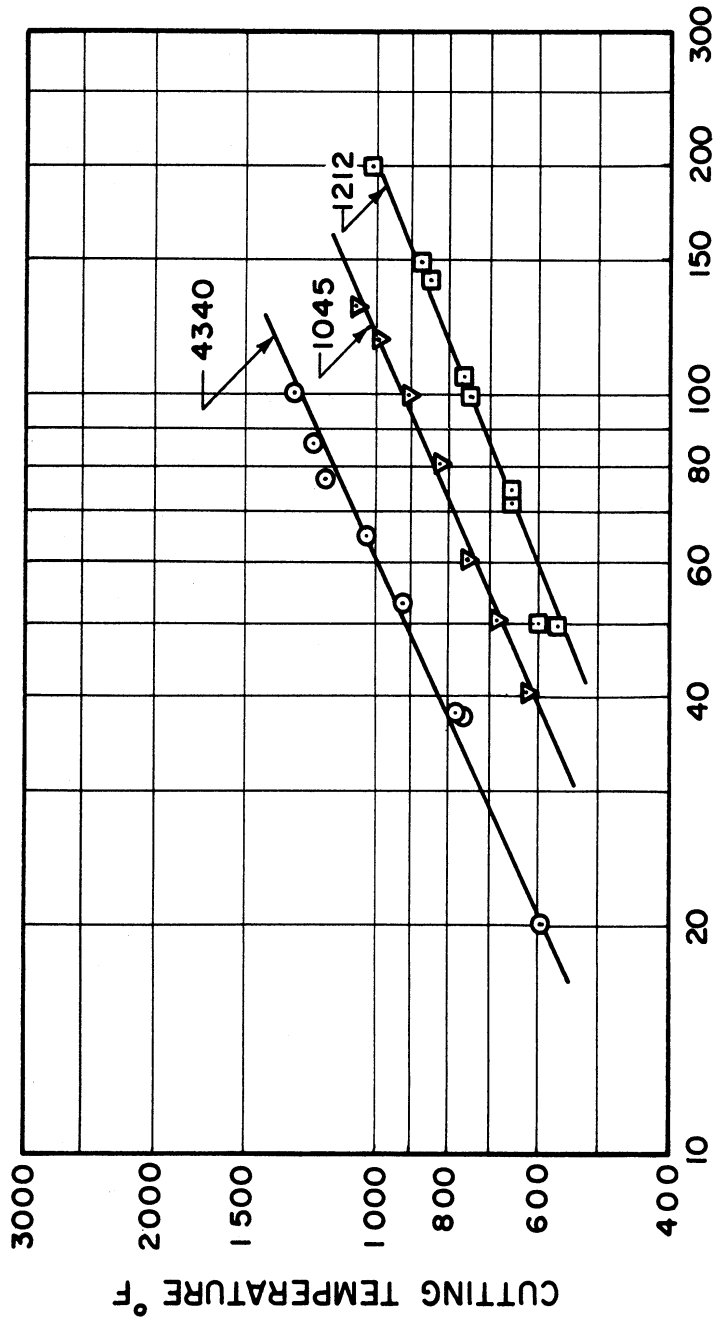

Figure 28. Tool Chip Interface Temperature. AISI 1212, 1045 and 4340 Steels.

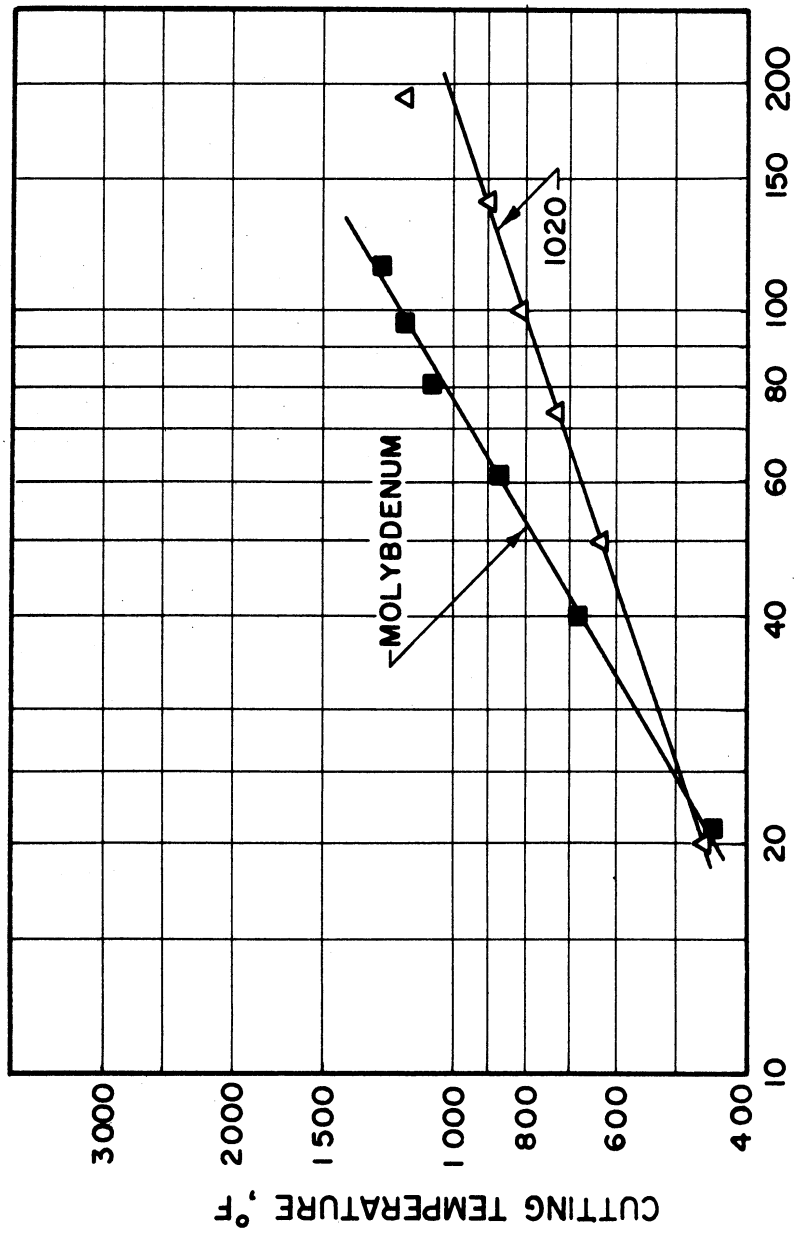

Figure 29. Tool Chip Interface Temperature.
AISI 1020 Steel and Molybdenum.

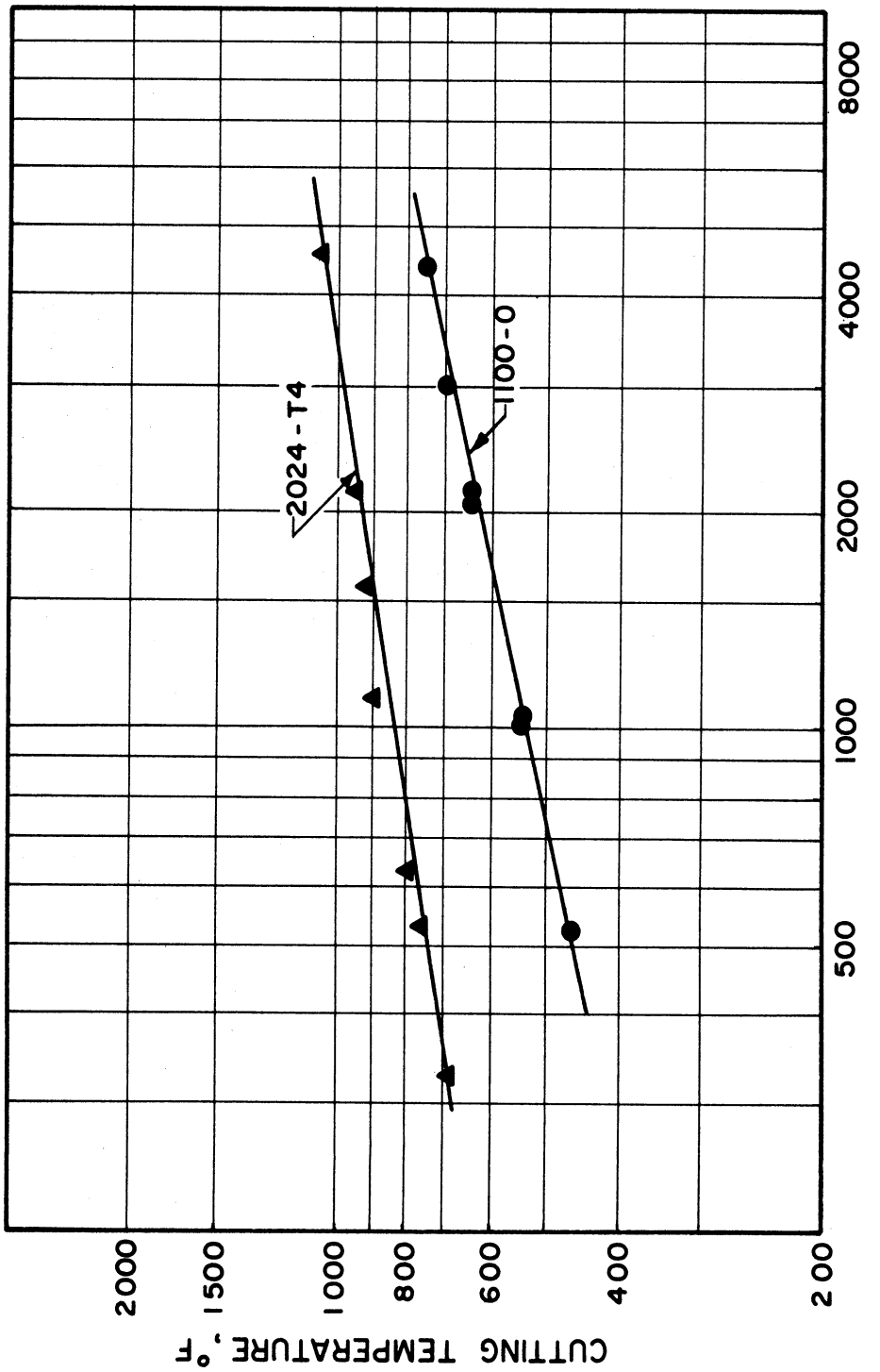

Figure 30. Tool Chip Interface Temperature. 1100-0 and 2024-T4 Aluminums.

TABLE IX

CUTTING TEMPERATURE CONSTANTS

Material	Constants[1] A	a	Velocity Validity V_L^2	Range V_u^3
	°F		FPM	FPM
AISI 1020	154	0.36	20	180
AISI 1212	105	0.43	50	200
AISI 1045	116	0.48	40	150
AISI 4340	144	0.47	20	120
Al 1100-0	118	0.22	500	5000
Al 2024-T4	275	0.16	300	5000
Molybdenum	71	0.61	20	120

1. $\theta = AV^a$

2. V_L - lower limit

3. V_u - upper limit

Abrasive Wear Testing

Wear tests were conducted to examine the abrasiveness of the materials under study. The University of Michigan Friction Wear Machine[84] used in these tests, is described in detail in the above mentioned reference. The machine is basically a drill press, modified for the purpose of friction wear testing.

Many different geometries of wear specimens may be used. A combination of a sphere and a plane was chosen for this investigation since it facilitates obtaining the desired stresses without overloading the machine and essentially elminates alignment difficulties.

The test specimen, a spherical segment of the work material ground to 12 - 15 RMS surface finish, is described in Figure 31. The mating plane is a portion of the high speed steel tool bits used for the machinability tests, polished to facilitate wear measurements.

The contact stresses were computed according to Hertz,[85,86,87] and the results are given below.

The maximum compressive stress is given by

$$P_{max} = \frac{3N}{2\pi a^2} \tag{31}$$

$$a = \frac{3\pi NR}{4} (K_1 + K_2)^{1/3} \tag{32}$$

Substituting into Equation (31) the value of "a" from Equation (32), and the numerical values $\nu_1 = \nu_2 = 1/3$ and R = 5/8, we obtain;

$$P_{max} = \frac{3N}{2\pi} \left[\frac{12}{5N} \cdot \frac{E_2}{(E_2/E_1 + 1)} \right]^{2/3} = 0.856\, N^{1/3} \left[\frac{E_2}{E_2/E_1 + 1} \right] \tag{33}$$

$$N = 1.594\, P_{max}^3 \left[\frac{E_2/E_1 + 1}{E_2} \right]^2 \tag{34}$$

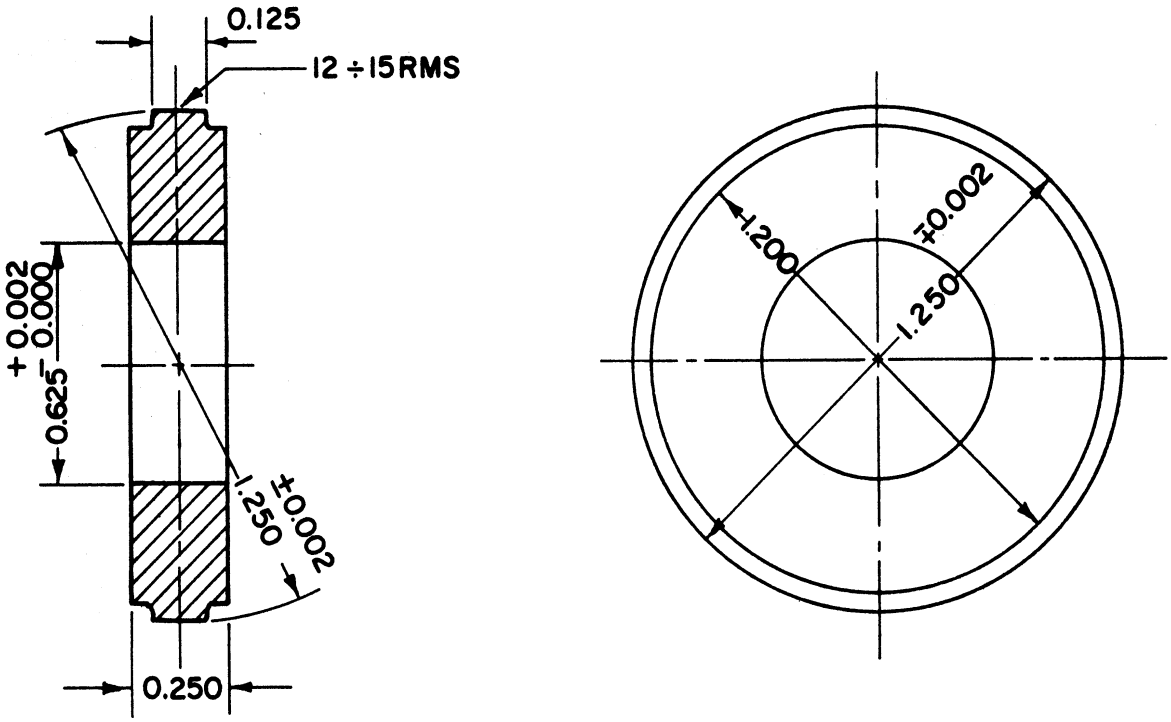

Figure 31. Wear Specimen.

Introducing the value $E_2 = 29 \times 10^6$ we get the final expression

$$N = 1.896 \left[\frac{P_{max}}{10^5}\right]^3 \left[\frac{E_2}{E_1} + 1\right]^2 \qquad (35)$$

NOMENCLATURE

a = radius of contact area

E = modulus of elasticity

$K = \frac{1-\nu^2}{E}$

N = normal load

P = compressive stress

R = radius of spherical speciman

ν = Poisson's ratio

Subscripts

1 = spherical specimen

2 = plane specimen

max = maximum

The values of the normal loads applied in the friction wear tests corresponded to an initial fictitious stress level of one and one half times the stress for a strain of 0.002 in./in. They are listed in Table X.

The friction wear tests were conducted dry, for periods of one (1), two (2) and thirty (30) minutes, at a nominal surface speed of 100 fpm. The wear patterns on the high speed steel tool bits were photographed with a grid superimposed upon them photographically. The area of the wear pattern was measured, and the volume of the wear products computed. This volume, as shown in Figure 32, is approximately proportional to the square of the area. Results are listed in Table XI. A sample of wear patterns is given in Figure 33.

Though it was thought, at the beginning of this study, that any attempt to predict machinability would require consideration of the abrasiveness of the work material, we have concluded later to the contrary. It is generally considered that the size, shape, amount and distribution of the second phase determines the mechanical properties as well as the abrasiveness of the material. From the tests conducted in this study, it appears that the effect of the second phase is taken care of sufficiently well by the mechanical properties.

Elevated Temperature Properties

Toward the end of this study it became obvious that it would be necessary to obtain high temperature properties of the work materials in order to be able to correlate the machinability with those properties. The room temperature properties, that we had obtained experimentally,

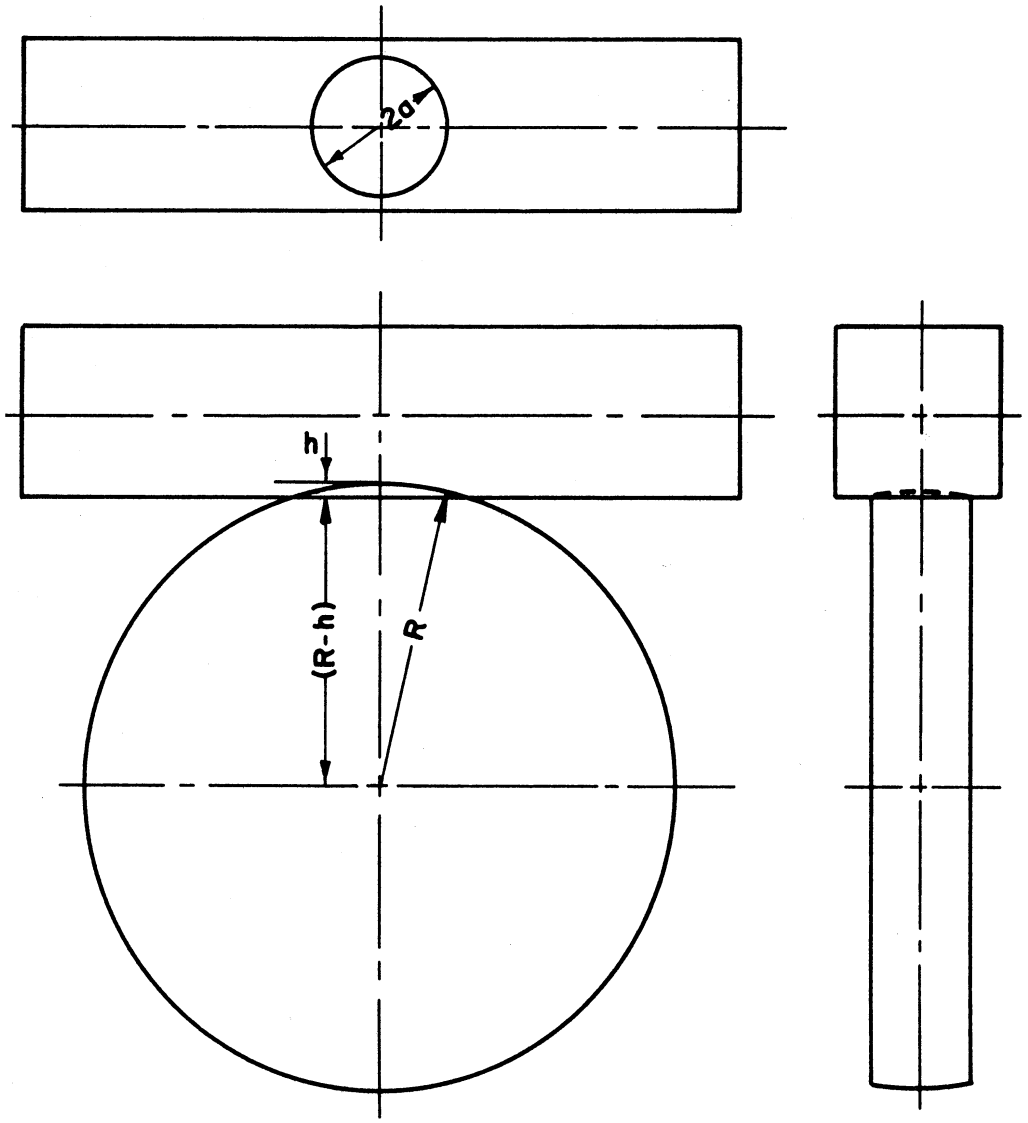

$$(R-h)^2 + a^2 = R^2$$

$$h \ll a$$

$$\therefore \quad h = \frac{a^2}{2R}$$

$$\text{VOLUME} : V = \frac{1}{6}\pi h(3a^2+h^2) \simeq \frac{1}{2}\pi a^2 h = \frac{\pi}{4R}a^4$$

$$\text{AREA} \quad : A = \pi a^2$$

$$\therefore V \approx A^2$$

Figure 32. Contact Geometry.

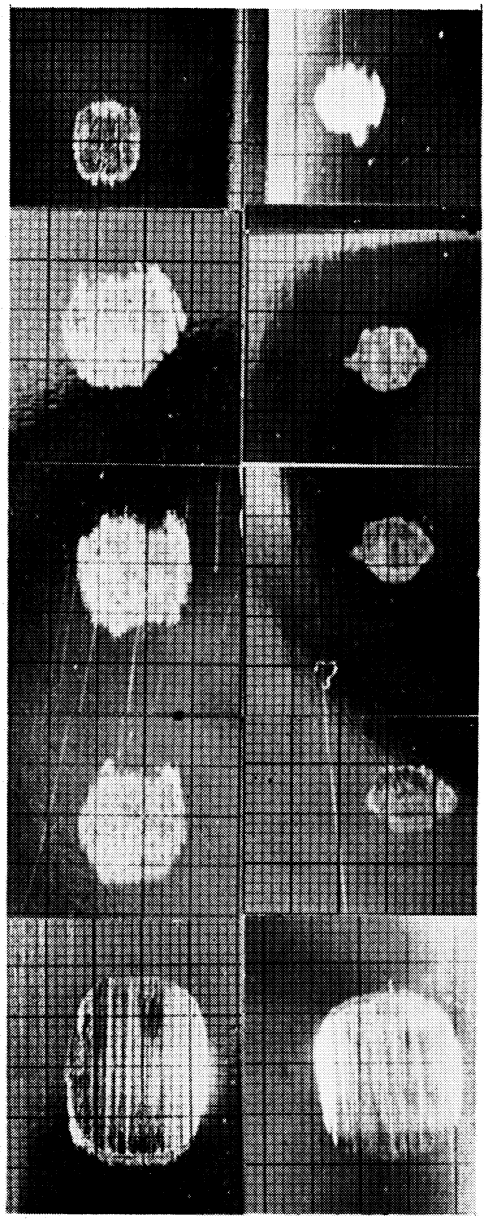

(a) (b)

Figure 33. Wear patterns, with grid superimposed (5.5X)

(a) AISI 4340 steel
(b) AISI 1045 steel

TABLE X

ABRASIVE WEAR MAXIMUM PRESSURES

AND NORMAL LOAD APPLIED

Material	Maximum Normal Pressure P_{max} psi	Normal Load Applied N lbs
1. AISI 1020	45×10^3	0.69
2. AISI 1212	37.5×10^3	0.40
3. AISI 1045	105×10^3	8.78
4. AISI 4340	180×10^3	44.23
5. Al 1100-0	9.8×10^3	0.03
6. Al 2024-T4	54.8×10^3	4.35
7. Molybdenum	70.5×10^3	1.57

TABLE XI

ABRASIVE WEAR TEST RESULTS

Material	Wear Time: 1 Minute — Area 10^{-4} in^2	Wear Time: 2 Minutes — Area$^{(1)}$ 10^{-4} in^2	Wear Time: 30 Minutes — Area 10^{-4} in^2
1. AISI 1020 Steel	12.4	4.1 - 12.4	43.0
2. AISI 1212 Steel	13.3	1.2 - 8.3	41.4
3. AISI 1045 Steel	39.8	29.0 - 36.5	172.2
4. AISI 4340 Steel	33.2	89.4 - 96.1	202.0
5. Al - 1100-0	6.6$^{(2)}$	(3)	90.5$^{(2)}$
6. Al - 2024-T4	4.1	1.7 - 5.0	3.3
7. Molybdenum	7.5	5.0 - 11.6	77.8

(1) Range for three tests.

(2) Excessive vibrations increase contact area.

(3) No two minute tests conducted.

served as a guide in the proper selection of the elevated temperature properties. Table XII gives the tensile strength, area reduction and thermal conductivity of the experimental materials at 600°F, the average temperature of the cutting zone. The Brinell Hardness was computed from the tensile strength by using experimental relationships. Table XIII gives the same properties for eighteen additional materials which were used to varify the general machinability equation.

TABLE XII

ELEVATED TEMPERATURE PROPERTIES OF MATERIALS TESTED IN THIS STUDY[1]

	Material	Tensile Strength σ_T psi	Area Reduction A_r %	Thermal Conductivity K Btu/Hr-Ft-°F	Brinell Hardness[7] H_B Kg/mm^2
1.	AISI 1020 Steel	58,000[2]	60	25.5[4]	116
2.	AISI 1212 Steel	53,000[3]	60[3]	28.0[4]	106
3.	AISI 1045 Steel	90,000[3]	35[3]	22.0[4]	180
4.	AISI 4340 Steel	135,000	40	18.5[4]	270
5.	Al-1100-0	2,800[5]	90[5]	115.0[3]	4.9
6.	Al-2024-T4	15,700[5]	65[5]	80.0[3]	27.5
7.	Molybdenum	85,000[6]	75[6]	66.0[6]	170

1. All properties at 600°F.

2. Whenever the reference is not given the data was taken from the Metals Handbook, 8th edition, ASM, 1961.

3. Estimated values from published data.

4. Austin, J. B., The Flow of Heat in Metals, ASM, 1942.

5. The Elevated Temperature Properties of Aluminum and Magnesium Alloys, ASTM, 1960.

6. Molybdenum Metal, Climax Molybdenum Company, 1960.

7. Brinell Hardness was computed from the Tensile Strength.

For steel and molybdenum $\sigma_T = 500\ H_B$

For aluminum $\sigma_T = 575\ H_B$

TABLE XIII

ELEVATED TEMPERATURE PROPERTIES OF THE MATERIALS USED TO VALIDATE THE GENERALIZED MACHINABILITY EQUATION[1]

	Material[2]	Tensile Strength σ_T psi	Area Reduction A_r %	Thermal Conductivity K Btu/Hr-Ft-°F	Brinell[15] Hardness H_B Kg/mm^2
1.	Rene 41	205,000[3]	15 - 30[4]	8.6[3]	410
2.	Ti-6 AL-4V	112,000[5]	62[5]	6.0[5]	224
3.	Ti-155 - A	120,000[5]	48[5]	6.2[5]	240
4.	Udimet 500	175,000[6]	15	8.5	350
5.	Inconel X	155,000	34	11.9	310
6.	301 Stainless Steel	70,000[7]	40[4]	12.4	140
7.	303 Stainless Steel	72,000	53	11.9	144
8.	310 Stainless Steel	50,000[8]	55[8]	9.9[8]	100
9.	347 Stainless Steel	62,000[8]	32[8]	11.1[8]	124
10.	410 Stainless Steel	73,000	74	15.6	146
11.	430 Stainless Steel	64,000	75	14.4	128
12.	446 Stainless Steel	83,000	40	13.2	166
13.	Fe-Cr-Mo Alloy	88,000[9]	60[4]	16.0[9]	176
14.	Zirconium	30,000[10]	66[10]	10.7[10]	75
15.	Armco Iron	32,000[4]	85[4]	32.0[10]	64
16.	Gray Cast Iron	* (12)	1-5[4]	32[14]	105[16]
17.	Pearlitic Cast Iron	* (12)	1-5[4]	26[4,13]	192[16]
18.	Leaded Read Brass	29,000	15[4]	41	58

FOOTNOTES

1. All properties at 600°F.

2. Materials used to varify the validity of the General Machinability Equation.

3. Engineering data VM-107, Rene 41, General Electric Company (1958).

4. Estimated Values from published data.

5. Bulletins No. 1 and No. 5, Titanium Metal Corporation of America. (1957 and 1958).

6. Whenever the reference is not given the data was taken from the Metals Handbook, 8th Edition, ASM, 1961.

7. All Stainless Steel data, unless otherwise stated, is from Alleghany Ludlum Steel Corporation, Data Sheets, 1957.

8. Haynes Stellite Company, Data Sheet 1958.

9. Alloy Casting Institute, Data Sheets, 1957.

10. Zirconium Data File, Carborundum Metals Company.

11. Austin, J. B., "The Flow of Heat in Metals," ASM. 1942.

12. No tensile strength value given.

13. McAdams, W. H., Heat Transmission.

14. Jakob, M., Heat Transfer, VI, 1956.

15. Brinell Hardness was computed from the Tensile Strength.

$$\text{All material except Zirconium } \sigma_T = 500\ H_B$$
$$\text{for Zirconium } \sigma_T = 400\ H_B$$

16. Measured values.

IV. DIMENTIONAL ANALYSIS AND THE GENERAL MACHINABILITY EQUATION

This chapter is divided into three areas: the development of the general machinability equation; a study of the effect of the size of cut on the cutting velocity for a constant tool life; and a brief analysis of the cutting speed-tool life relationship.

The Development of the General Machinability Equation

Metal cutting is basically a plastic deformation process, where the material is locally deformed to fracture. It is accompanied by unavoidable high friction, both on the tool face between the tool and the chip, and on the flank between the tool and the machined surface. Both the deformation energy and the energy dissipated in friction is transformed into heat. Most of the heat is carried away by the chips, part is conducted to the work piece, and portions of lesser significance are conducted through the tool and carried away directly to the atmosphere. The process is essentially a steady state process within a few seconds after cutting begins.(88)

The prediction of the behavior of a material in a cutting process, even under the idealized conditions of a two dimensional cut as shown in Figure 2 is a complex problem. It requires that the influencing physical properties of the material being cut be reliably known. Inasmuch as all materials are made to a specified range of physical properties, any machinability analysis therefore will be only as accurate as the physical property data on which it is based.

This dissertation is concerned with the study of the effect of the physical properties of the work material on machinability, where

machinability is defined in terms of tool life. Obviously machinability is also a function of the tool material and geometry, the cutting conditions and the atmosphere in which the process is taking place. To restrict the problem, as far as possible, the tool material and geometry, as well as the cutting atmosphere were fixed for this investigation. This does eliminate the variablesassociated with the tool and the surroundings as variables, and enables us to place all of our attention to the subject of our investigation: the effect of the work material properties on machinability. We further fixed the depth and width of cut to minimize experimental work. Sufficient data concerning the effect of the size of cut on tool life is already available in the literature to check any relationship under question.

The dimensional analysis[89] is a very powerful tool to study the effect of the different independet variables effecting any physical phenomenon. It enables us to capitalize on partial knowledge of the physical situation. The nature of the fundamental laws which govern the system, and the boundary conditions have to be known and understood. It is not necessary to be able to express them in the form of mathematical equations.

The Pi Theorem, or rephrased to express the "Principle of Dimensional Homogenity" as stated explicity by E. Buckingham[90] in 1914 but used already implicitly by Baron Jean Baptiste Fourier is the basis of that analysis.

The dimensional analysis as a tool simplifies appreciably the experiment, by reducing the actual number of variables in the test, and by giving more freedom in changing those variables that can be controlled most readily. It provides a functional relationship between the variables

and helps to correlate the experimental data.

As every other tool, it has its limitations. Firstly, all the independent variables affecting the process have to be known. Secondly, the analysis does not provide directly any explanation about the mechanisms involved in the phenomenon under study. And thirdly, there is a big flexibility in the choice of the dimensionless groups.

It seems that the first of these limitations is generally true for any analysis, the second is true for any study using the phenomenological approach, and the third, rarely mentioned as a limitation, should be of most concern. Choosing the "right" groups may lead to the understanding of the process.

Applying the Pi Theorem to the problem under consideration, a number of dimensionless groups are generated equal in number to the difference between the total number of variables and the number of arbitrarily chosen primary variables: Length (L), Time (T), Mass (M), and Temperature (θ). The process is mechanical, undiscriminatory, and different dimensionless groups may be obtained, some of which are significant, others being completely meaningless. To which of the two classes any one dimensionless group belongs, can be determined only on physical grounds, by understanding the phenomenon.

Table XIV lists seven independent variables, and the tool chip interface temperature θ as a dependent variable. A discussion of the completeness of this list, the significance of the variables, and why other variables, seemingly influencing the process were not included would be appropriate at this time.

TABLE XIV

VARIABLES FOR DIMENSIONAL ANALYSIS

Variable	Dimension	Description
H_B	$ML^{-1} T^{-2}$	Brinell Hardness (Kg/mm^2)
A_r	None	Reduction in Area
ρC	$ML^{-1} T^{-2} \theta^{-1}$	Volume Specific Heat (Btu/Ft^3 -°F)
K	$MLT^{-3}\theta^{-1}$	Thermal Conductivity (Btu/Hr -Ft -°F)
t	L	Depth of Cut (in)
w	L	Width of Cut (in)
V	LT^{-1}	Cutting Velocity (Ft/min)
θ_f	θ	Tool Chip Interface Temperature (°F)

It appears to the writer that all of the parameters that characterize the metal cutting process, like cutting forces, coefficient of friction between the chip and the tool, "shear" angle, tool life, chip ratio, etc., are dependent variables. Some of them were considered as independent variables by previous researchers, others taken as dependent ones. None of these parameters may be predicted on the basis of todays theory, and most of them will have to be evaluated experimentally for many years to come. Further development of the theory of plasticity, and a better understanding of the chip forming mechanism, is a major prerequisite for any serious solution to the deformation problem in metal cutting.

Based on our studies it was found after investigating all of the mechanical properties that the hardness and the area reduction completely describe the plastic behavior of the metal for prediction of machinability. It is interesting to note that Herbert[91], in the 1920's, came to the conclusion that "the measure of the machinability is the hardness of the chip".

Hardness "in general implies resistance to deformation", as D. Tabor states in the introduction to his book "Hardness of Metals".[92] The range of elastic deformation for metals is relatively small, therefore the hardness is influenced primarily by the plastic properties of the material, the plastic modulus, σ_o, and the strain hardening index m in the equation $\sigma = \sigma_o \epsilon^m$. Figure 34 shows a typical stress strain diagram. Hardness as has been learned recently provides adequate information about the plastic portion of the stress-strain diagram but does not indicate its end point. To this extent it is equivalent to the "tensile strength" or the "compressive strength", and they could be interchanged in our analysis.

It is obvious from Figure 34, that to complete the information about the mechanical properties of the material, a variable describing the ductility of the material has to be introduced. This variable has to be descriptive of the maximum strain the material can endure, or as the metal cutting researcher prefers to look at it, the minimum strain required to cause fracture ϵ_f . The relations between area reduction (A_r), fracture strain ϵ_f and the area ratio (R_f) are given below, so that any one of them may be used in our analysis freely.

$$A_r = \frac{A_o - A_f}{A_o} \times 100 \tag{36}$$

$$_f = \ln A_o/A_f = \ln R_f \tag{37}$$

$$\frac{100 - A_r}{100} = \frac{1}{R_f} \tag{38}$$

Where A_o is the original area of the cross section of a tensile specimen and A_f the final area.

To characterize the effect of the thermal properties on the metal cutting process the volume specific heat ρC (Btu/Ft^3 -°F) and the thermal conductivity K, (Btu/Hr - Ft - °F) should suffice. This statement is true, provided the heat transfer through the tool, and the heat conveyed to the surrounding is of second order importance. Experimental evidence by Schmidt[93], Pahlitzsch[94], Danielian[95], and Vierrege[96] varify that assumption for dry cutting condition.

The cutting conditions, depth of cut t (in) , width of cut w (in) and cutting velocity V (ft/min) conclude the list of independent variables.

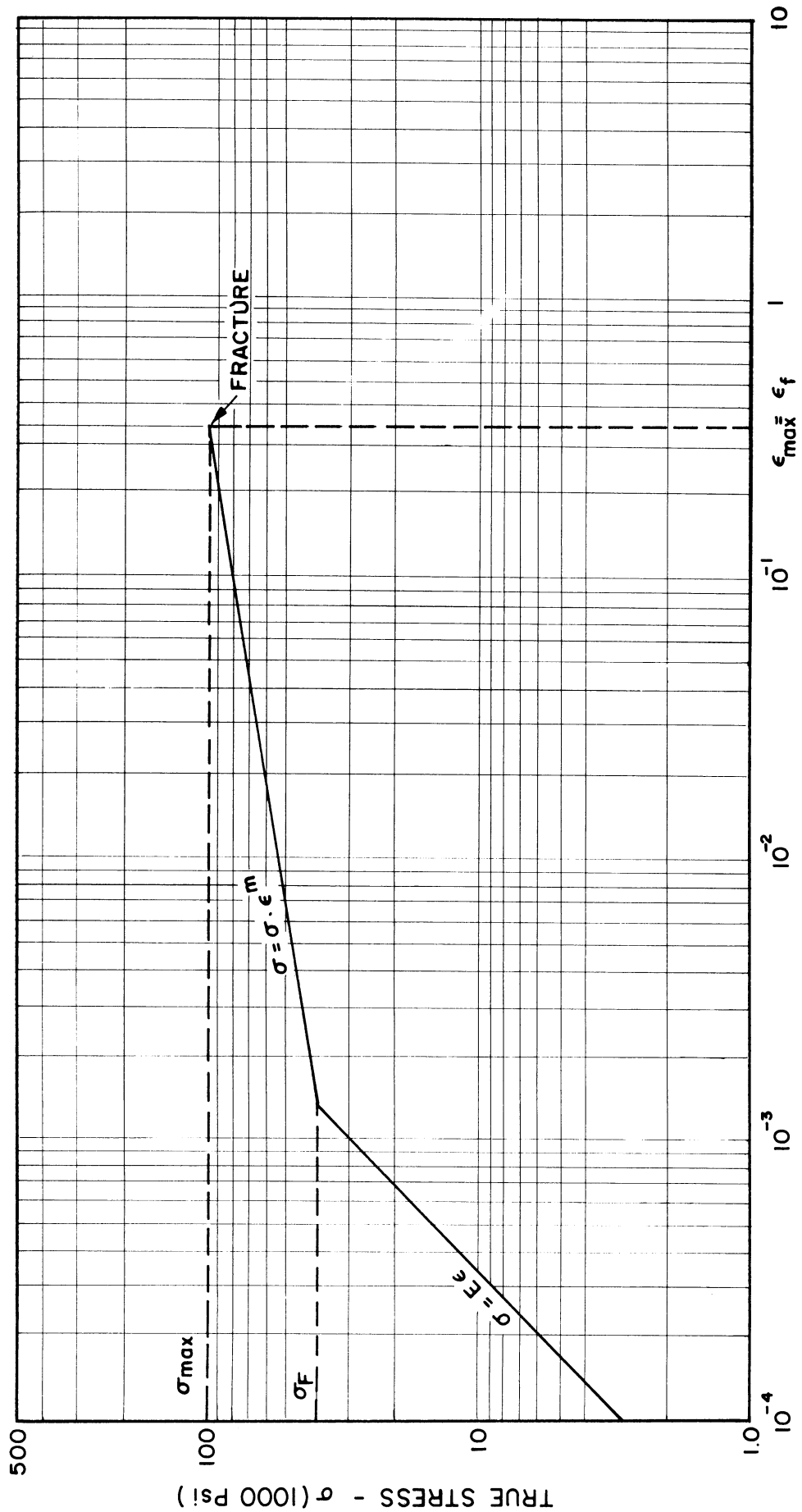

Figure 34. Typical True Stress Strain Diagram.

Other variables were considered and found, either to be dependent on variables already considered, or of second order signifance.

For instance, it was assumed that consideration should be given to the presence of the second phase, in particular to its abrasive effect on the wear of the tool. Experimental work showed that this effect is well taken care of in the mechanical properties. After all, these properties are as much a function of the second phase as they are of the first phase. The coefficient of friction can serve as another example of a dependent variables, therefore should not be in our list.

Moduli of Elasticity are considered of second order significance for reasons brought out above. Strain rate effects, are by far less significant than most metal researchers postulated[97], [98]. The analysis of the metal deformation, as being a shear phenomenon occurring in a very narrow region, led to the conclusion that the strain rates are extremely high. Our own work shows that the deformation happens in a much wider region, consequently yielding lower strain rates, and though they are still large their effect on the process is of second order.

The average tool chip interface temperature θ_f was chosen as the dependent variable. Based on our experimental work presented in Figures 28, 29, and 30, showing the cutting temperature versus the cutting velocity, this temperature was found to be $975 \pm 25°F$ for a cutting velocity V_{60}, correspondint to a sixty minutes tool life. It will not be necessary therefore to have time in the generalized machinability relationship. The velocity for a sixty minute tool life will therefore be that velocity that gives an average tool chip interface temperature of 975°F.

On the basis of the above discussion we whould look for four dimensional groups. After much deliberation the following four were selected: (Vw/α); (w/t); $(C\rho\Theta_f/H_B)$ and R_f, where R_f was defined above as

$$R_f = A_o/A_f \text{ , or } \frac{100 - A_r}{100} = \frac{1}{R_f} \text{ ,}$$

α is the thermal diffusivity defined as

$$\alpha = K/\rho C \text{ .}$$

K is the thermal conductivity, ρ is the density, and C is the specific heat.

Before coming to this final conclusion we have considered many different variables, consequently we had many other dimensionless groups, some of which will be discussed here.

The effect of the ratio between the yield strength (σ_y) and the tehnsile strength (σ_T) was examined. Though Janitsky[72] built his machinability index for steels on the ratio (σ_y/σ_T) it was not found to have general validity.

$(\rho V^2/q)$ or $(\rho V^2/\sigma_y)$, where (ρV^2) could be considered as an inertia stress is a dimensionless group, discussed by Drucker[99] and others was dropped, knowing that inertia forces are insignificant in convensional machining speeds[100] since $\rho V^2 << \sigma_T$.

Groups like $(T_L V/\sqrt{F})$, of which Kronenberg[101] makes use were dropped on the basis that the effect of the depth and of the feed are not interchangeable, though the area of the cross section (F) remains the same.

An attempt was made to make use of a group like $(\theta_f^2 / H_B^2 \cdot K\rho C/Vt)$, including $(K\rho C)$, which was claimed by Shaw et al.[102] to be very significant. Unfortunately the experimental data did not follow any specific pattern when plotted in this fashion.

To conclude the discussion about those dimensionless groups that are included in this analysis, we would like to mention that many more groups were considered, some of them ratios or multiplication of others, physically they could not be interpreted, and experimentally they did not provide the expected correlation.

The first group that was found to be significant is the thermal number (Vw/α) the importance of which was recognized by Bisacre[103] and Chao[37] and later by others[104]. The thermal number was interpreted as the ratio of the transit time over the relaxation time[103]. More specifically to the metal cutting it governs the ratio of the heat conducted through the work to the heat convected by the moving chip.

The second group or the area ratio R_f, becomes larger the higher the ductility of the material. The larger the ductility, keeping all other variables constant, the lower we would expect the machinability to be inasmuch as the ductility determines the area under the stress strain curve which is a measure of the work done during machining. In the limit, when $A_r = 100\%$, $R_f = \infty$, or in words, when the material can withstand an infinitely large strain, we should not be able to machine the material at all.

The third group $(C\rho\theta_f/H_B)$, where $(C\rho/H_B)$ could represent a temperature raise, if all the heat is carried away with the chip, and none whatsoever is conducted away.

The fourth group (w/t), where w is the width and t the thickness, represents the geometry of the cut and does not need any further elaboration.

It follows that

$$Vw/\alpha = A(w/t)^a \left(\rho C\Theta_f/H_B\right)^b (R_f)^c , \tag{39}$$

or if t and w are constants

$$V/\alpha = A_1 \left(\rho C\Theta_f/H_B\right)^b (R_f)^c \tag{40}$$

To evaluate the constants in this equation the properties of the experimental materials as well as the corresponding velocity and temperatures were used. In order to evaluate the machinability of the various materials it is necessary to select one set of standard conditions to serve as a basis. A very logical basis, one that has been very often used in the past, is the cutting speed that results in a 60 minute tool life, and is designated as V_{60}. Experimental data on all of the materials studied in this project as well as some additional data found in the literature indicates that this also corresponds to one value of tool-chip interface temperature, which is about 1000°F for a 60 minute tool life. This limiting temperature is higher for a shorter tool life and is proportionally lower for tool lives in excess of 60 minutes.

One further problem in this same category is the determination of the temperature at which the physical properties of the material should be evaluated. After examining carefully movies of the metal deformation in the cutting zone, it is apparent that most of the deformation occurs in

a region where the temperature is about 600°F. On the basis of this observation, it was decided that all the physical properties of the material should be evaluated at 600°F.

Using the properties of the material at 600°F, the cutting velocities corresponding to a sixty minute tool life, and the postulate that the temperature is for all practical purposes constant for these speeds, the numerical value of the exponents b and c are found to be 1.0 and -0.5, respectively.

Substituting the values in Equation (40) and lumping all constants into one constant A_2 we get:

$$V/\alpha = A_2 \frac{\rho C}{H_B} R_f^{-1/2} \tag{41}$$

Where $A_2 = 1150.$

V_{60} in FPM can be expressed explicitly as

$$V_{60} = A_2 \frac{K}{H_B R_f^{1/2}} \tag{42}$$

since $\alpha = K/\rho C$, and ρC can be cancelled on both sides of the equation.

Inasmuch as most handbooks list the area reduction rather than the more convenient area ratio, Equation (42) can be rewritten as

$$V_{60} = A_2 \frac{K}{H_B} (1-A_r/100)^{1/2} \tag{43}$$

substituting the value of A_2 yields:

$$V_{60} = \frac{1150K}{H_B} (1-A_r/100)^{1/2} \tag{44}$$

This relationship enables us for the first time and by means of simple calculations, to orderly arrange the materials and predict their machinability on the basis of three of their physical properties: thermal conductivity K (Btu/Hr - Ft - °F) , area reduction A_r and Brinell Hardness H_B (Kg/mm^2). The constant A_2 is computed from the various standard units used.

Figure 35 shows this relationship graphically, with the experimental points on the graph. It is immediately obvious that the 2024-T4 aluminum and the molybdenum do not fit the curves. As a matter of fact, it would be strange if they did. For the 2024 aluminum, the melting range is 935 - 1180 °F, and for a 1000°F interface temperature it would be expected that localized melting would occur at the grain boundaries, accompanied by a sharp decrease in the ductility and some reduction of the hardness. Therefore the machinability will obviously be better than predicted on the basis of the general machinability equation.

As to the molybdenum, the micrograph of the chip, as shown in Figure 36, explains best why the material deviates from the expected behavior. Two observations can be made. First, the material fails through the grain boundaries with cracks forming in the material ahead of the tool, separating the metal being deformed by means of an insulting void space from the bulk of the work piece. Second, the material continues to undergo great deformation as the chip is formed.

Most of the molybdenum carbides (Mo_2C), the hardness of which is between 1400 and 1800 Vickers, are located at the grain boundaries, and consequently these hard carbides will be in contact with the tool.

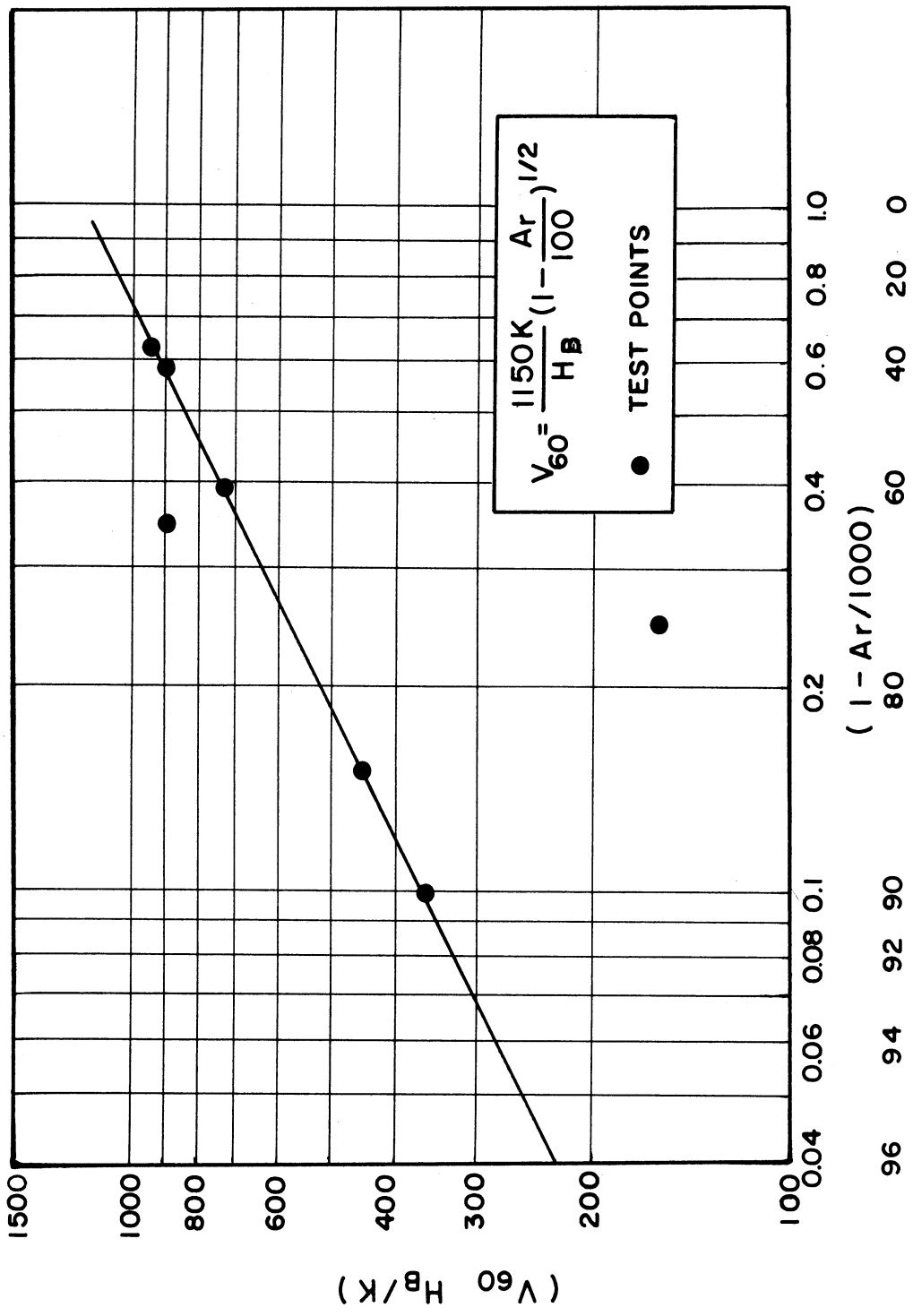

Figure 35. The General Machinability Equation.

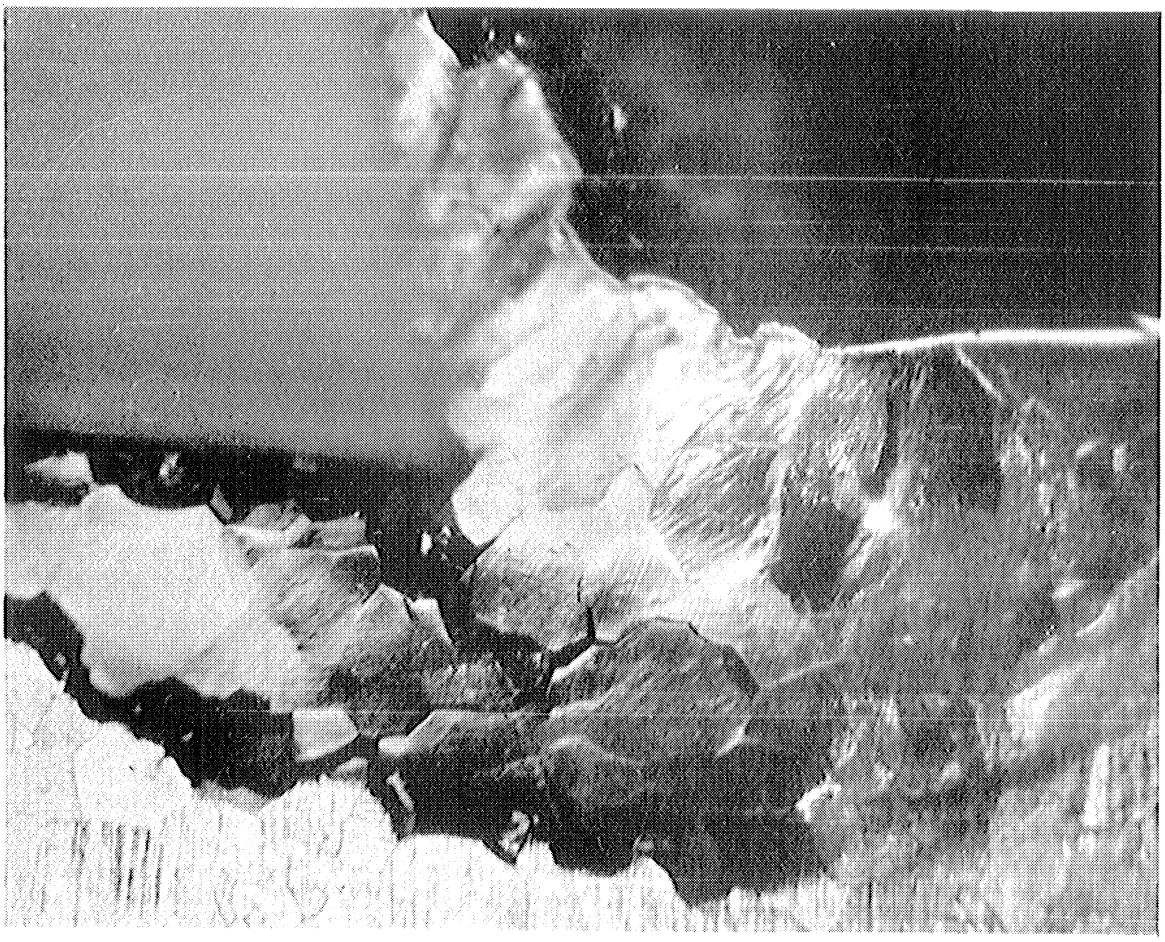

Figure 36. Chip Formation in Molybdenum Cutting Velocity = 0.020 ipm, Depth of Cut t = 0.010 in, Width of Cut w = 0.100 in, Rake Angle 10°.

Their effect on the wear will be by far larger than their effect on the hardness of the work material. The cracks formed effectively insulate the cutting zone from the work material and consequently the effective thermal conductivity is much smaller, probably by a factor of three to four. As to the ductility on the small, the deformation in the chip shows that it was essentially not effected. If we sum up these factors, it is obvious why the actual sixty minute cutting velocity is so much lower than the predicted one.

To validate the general machinability equation comparison is made with data published by different research institutes, technical societies and recommendation of the manufacturers. Table XV gives the predicted values of machinability in terms of V_{60} for a variety of materials. It verifies clearly the validity of the relationship for materials as different as cast iron, steel, aluminum, zirconium and titanium, as well as for nearly similar materials, as 1020, 1045, 4340 and 1212 steels or the stainless steels.

The final machinability relationship stated above can be used with the following qualifications:

1. The predicted machinability values are no more accurate than the properties that are used to compute them. Exactly as the measured value of the area reduction may vary from one specimen to another of the same material by 50% or more so may the machability vary by as much as $\sqrt{2}$, as any metal cutting researcher knows.

2. The material should not have any critical transition temperature below 1000°F. If it does, it is necessary to go back to the first basic relation and select different temperatures and properties associated with them.
3. The hardness of the material should be at least 100 Brinell hardness numbers lower than that of the tool.
4. The numerical value of V_{60} is for a T-1 high speed steel tool, with 0,0,7,7,7,0,0, tool designation, depth of cut $t = 0.0057$ in., width of cut $w = 0.050$ in., and cutting dry.

The effect of variables other than the physical properties, such as the cutting conditions, are discussed in the following two sections.

The Effect of the Size of Cut on the Cutting Velocity for Constant Tool Life

Different approaches were used in the past to consider the effect of the dimensions of the cut on machinability. Woxen[105] introduced a "chip equivalent" q', defined as $q' = t+w/wt$, and considered the cutting velocity as some function φ of q'; $V = \varphi(C, q', T_L)$, where C is a constant depending on the cutting conditions and the material cut. q' was considered to inadequately represent the effect of the dimensions of the cut, for the simple reason that interchanging the depth and the width, will have no effect on q', but have a remarkable effect on the cutting velocity for a constant tool life.

Boston[106] states on the basis of his experimental work that an exponential relationship of form $V_{T_L} = Ct^{-x} w^{-t}$ exists, and describes

TABLE XV

PREDICTED MACHINABILITY VALUES

Material	Predicted V_{60} [1] FPM	Corrected V_{60} [2] FPM	Experimental V_{60} [3] FPM	Cutting Conditions
1. AISI 1020 Steel	158	160	160	Actual Test Value
2. AISI 1212 Steel	190	190	190	Actual Test Value
3. AISI 1045 Steel	113	120	120	Actual Test Value
4. AISI 4340 Steel	61	60	60	Actual Test Value
5. Al-1100-0	8650	8500	8500	Extrapolated Test Values
6. Al-2024-T4	1960[4]	2600	2600	Actual Test Values
7. Molybdenum	220[5]	60	60	Actual Test Values
8. Rene 41	20	17-20	50-60[6]	t=0.005; w=1/32; Carbide Tools[7]
			30-40	t=0.010; w=1/16-1/8; Carbide Tools
9. Ti-6 AL-4V	19	15-30	30-60[8]	HSS Tools, 15° Rake[9], Coolant[10], size of cut not specified
10. Ti-155-A	21	15-30	30-60[8]	HSS Tools, 15° Rake, coolant, size of cut not specified
11. Udimet 500	26	25	15[11]	t=0.009; w=0.100; 15° Rake, 48 minute tool life, 0.060 wear land; coolant
12. Inconel X	36	38	38	20% of V_{60} for AISI B1112 steel
13. 301 Stainless Steel	78	80	80[12]	Same conditions
14. 303 Stainless Steel	64	55-70	70-90[13]	Rough } Positive Rake[14], coolant, size of cut not specified
			80-130[13]	Finish }
15. 310 Stainless Steel	76	60-80	60-90	Rough
			100-120	Finish
16. 347 Stainless Steel	84	75-95	60-90	Rough
			100-120	Finish
17. 410 Stainless Steel	62	55-75	80-100	Rough
			100-130	Finish
18. 430 Stainless Steel	64	55-75	80-100	Rough
			100-130	Finish
19. 446 Stainless Steel	70	60-80	60-90	Rough
			90-120	Finish
20. Fe-Cr-Mo Alloy	66	55-75	80-100[15]	Finish cut, positive rake, coolant, size cut not specified
21. Zirconium	94	80-100	100-150[16]	t=0.005-0.010; w=0.010-0.040; positive rake, coolant
22. Armco Iron	220	225	225	Actual Test Value
23. Grey Cast Iron	340	350	270[17]	t=0.006; w=0.100
24. Pearlitic Cast Iron	150	155	120[17]	t=0.006; w=0.100
25. Leaded Red Brass	745	500-1000	385-1150[18]	150-600% of V_{60} for AISI B1112 Steel

FOOTNOTES

1. From the general machinability equation

$$V_{60} = \frac{1150\ K}{H_B}\ (1\text{-}A_r/100)^{1/2}$$

applying the data of Tables XII and XIII.

2. Cutting velocity corrected to our condition from values in (3).

3. Cutting velocities as recommended by industry and research institutions, and cutting conditions as specified by the source.

4. Prediction too low owing to localized melting in grain boundaries as explained in text.

5. Prediction too high owing to failure in grain boundaries, exposures of the molybdenum carbides, and effective insulation of the chip.

6. Engineering data VM-107, Rene 41, General Electric Company 1958.

7. Cutting velocity for one hour tool life is about three times as large for carbide tools as for high speed tools.

8. Bulletin No. 1 and No. 5 Titanium Metal Corporation of America (1957 and 1958).

9. Positive rake has a large effect on machinability of ductile material and negligible effect on machinability of brittle materials.

10. Coolant reduces the cutting temperature, in turn increasing the cutting velocity for any one tool life.

11. Metal Progress Data Sheet, 98 B, August 1961.

12. Titanium Reports, University of Michigan, 1953.

13. All stainless steel data taken from Metals Handbook, 8th edition, 1961.

14. Cutting conditions for all stainless steels are the same.

15. Alloy Casting Institute, Data Sheets, 1957.

16. Zirconium data file, Carborundum Metals Company.

17. Previous experimental work of Professor Datsko.

adequately the effect of the dimension of the cut on the cutting velocity for any tool life T_L. He cites the following particular relationships:

For steel: $$V_{90} = C_1 t^{0.61} w^{0.36} \quad (45)$$

For cast iron: $$V_{90} = C_2 t^{0.53} w^{0.23} \quad (46)$$

Where C_1 and C_2 are constant of different values for the different steels and cast irons.

Merchant and Ernst[107], in the Tool Engineers Handbook, state that in general $V = Ct^{0.77} w^{0.37}$.

The data compiled by the ASME Research Committee on Metal Cutting is reproduced in Figures 37 and 38. The curves show the correction factors for the velocity of a sixty minute tool life, as affected by a change in the dimensions of the cut. The curves represent all the data in the Manual on Cutting of Metals[108]. The exponents in this case are 0.62 and 0.36 for t and w respectively.

To consider the effect of the size of cut it is necessary to look at the two groups (Vw/α) and $(t/w)^a$ containing the dimensions of the cut; the depth t and the width w.

We may introduce a "Characteristic Length" q, which will include the effect of t and w in the following manner:

$$(Vw/\alpha)\ (t/w)^a = (V/\alpha)\ w^{1-a}\ t^a = (V/\alpha)\ q \quad (47)$$

where

$$q = w^{1-a}\ t^a \quad (48)$$

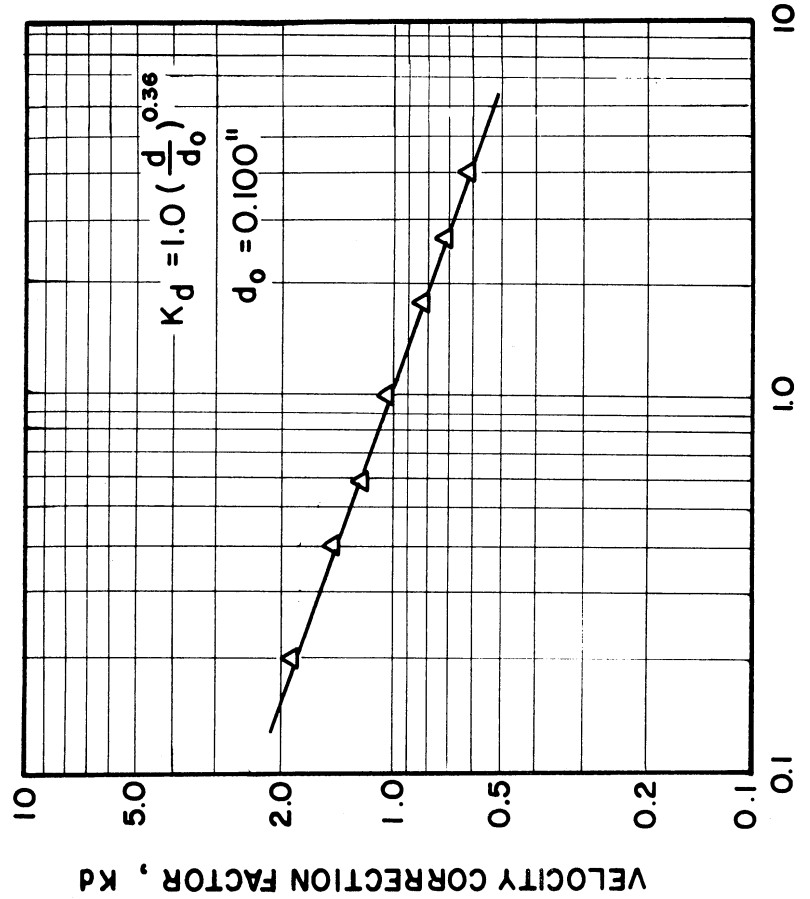

Figure 38. Effect of Depth of Cut on Cutting Velocity for a Sixty Minute Tool Life.

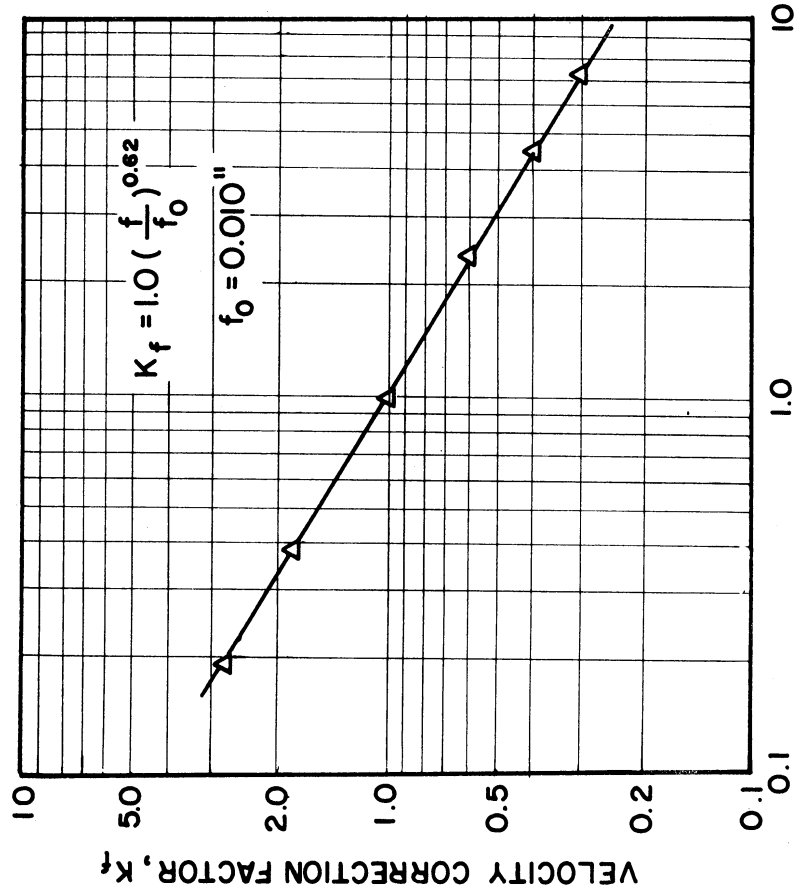

Figure 37. Effect of Feed of Cut on Cutting Velocity for a Sixty Minute Tool Life.

Based on all the experimental evidence mentioned above we can conclude that "a" is about two third ($a = 2/3$) for $0.1 \leq t/w \leq 0.2$, and therefore:

$$q = w^{1/3}\, t^{2/3} \tag{49}$$

From physical considerations and experimental results we know that "a" is not a constant, but varies with the ratio of the depth of cut to the width of the cut (t/w). When t = w, or their ratio is equal to unity, obviously the effect of both sould be alike, "a" will be equal to one half ($a = 1/2$) and $q = w^{1/2}\, t^{1/2}$. But when the ratio (t/w) goes to zero, the limit of "a" should be unity. Mathematically expressed:

$$\lim_{(t/w)\Rightarrow o} a = 1 \tag{50}$$

from which it follows:

$$\lim_{(t/w)\Rightarrow o} q = t \tag{51}$$

Table XVI, sums up the corresponding values of "a" and "q" for different (t/w) ratio. Figure 39. supplements this table.

TABLE XVI

RELATIONSHIP BETWEEN THE GEOMETRY OF CUT AND THE "CHARACTERISTIC LENGTH"

t/w	a	q in
0	1	t
0.15	2/3	$t^{2/3}\, w^{1/3}$
1	1/2	$t^{1/2}\, w^{1/2}$

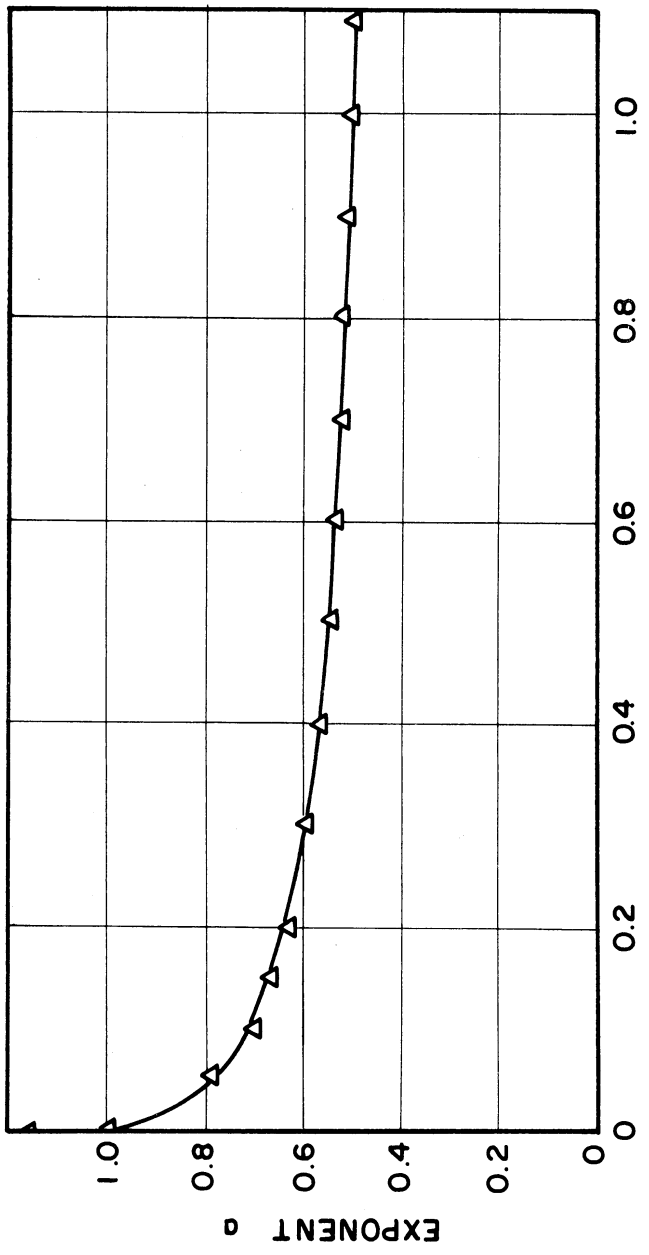

Figure 39. Chip Geometry Exponent "a"

Appendix B shows the results of a test conducted with a different depth of cut t and width of cut w to verify the above concept. It shows the validity of the postulated effect of q on V_{60}.

Tool Life Velocity Relationship

In general the tool life cutting velocity follows the exponential Taylor[7] relationship, $VT^n = C$, where n and C are constants depending on the tool, the cutting conditions and the material machined. The relationship is valid over the range of cutting velocities, which yield practical tool lives. For high speed steel tools, in general $0.05 < n < 0.15$, though it may vary over wider ranges. Taking an average of $n = 0.10$, will give reasonably good predictions for the cutting velocity for tool lives different from sixty minutes. The error in predicted cutting velocity is smaller than 5.5% if tool life is between 20 minutes and three (3) hours. The error is still less than 11% if the tool life range is extended to eight (8) hours. It should be mentioned that the smaller the value of n, the more sensitive is the tool life to the cutting velocity. In the extreme cases, for very small values of n, any error is objectionable, and it is necessary to resort to measuring the tool life.

V. CONCLUSIONS

1. A functional relationship was developed between the physical properties and machinability.
2. The Brinell Hardness (H_B) and area reduction (A_r) were found to describe adequately the effect of the mechanical properties on machinability.
3. The thermal conductivity (K) was found to describe adequately the effect of the thermal properties on machinability.
4. All material properties should be evaluated at the average temperature in the cutting zone.
5. The effect of the abrasiveness of the second phase on machinability is well taken care of by considering the mechanical properties of the material.
6. Abrasive wear tests could not be used to improve the prediction of the machinability of a material.
7. No relationship could be established between machinability and eithe impact strength, deformatin energy or the strainhardening exponents.
8. No relationship could be established between the chip hardness and machinability.
9. For a sixty minute tool life with a T-1 tool material the average tool chip interface temperature is $975 \pm 25^\circ$ °F, and the average temperature of the cutting zone is about 600° F.

10. The cutting velocity (V_{60}) for a sixty minute tool life is given by:

$$V_{60} = \frac{1150\ K}{H_B}\ (1-A_r/100)^{1/2} \qquad (52)$$

Cutting conditions are: T-1 High Speed Steel Tool, having the ASA shape 0,0,7,7,7,0,0,

Depth of cut $t = 0.0057$ in.

Width of cut $w = 0.050$ in.

Cutting Fluid - air

The machinability relationship is valid provided that:

a) The work material has no critical transition temperatures below the tool chip interface temperature.

b) The hardness of the work material is at least 100 Brinell Hardness numbers below the hardness of the tool.

APPENDIX A

SAMPLE CALCULATION OF TOOL LIFE RELATIONSHIP FOR AISI 4340 STEEL

	Cutting Velocity V FPM	Tool Life T_L min.	ln V y	ln T x	$(\ln T)^2$ x^2	$(\ln T)(\ln V)$ xy
1	70.0	2.8	4.24850	1.02962	1.06012	4.37434
2	60.0	34.0	4.09435	3.52637	12.43529	14.43819
3	65.0	19.6	4.17439	2.97553	8.85378	12.42102
4	70.0	1.75	4.24850	0.55962	0.31317	2.37755
5	80.0	1.3	4.38203	0.26236	0.06883	1.14967
6	75.0	1.6	4.31749	0.47000	0.22090	2.02922
7	55.0	27.5	4.00734	3.31419	10.98386	13.28109
8	85.0	0.75	4.44266	-0.28769	0.08277	-1.27811
9	60.5	106.0	4.10265	4.66344	21.74767	19.13246
10	65.3	53.0	4.17900	3.97030	15.76332	16.59188
11	67.5	9.4	4.21213	2.24071	5.02078	9.43816
12	70.5	8.3	4.25562	2.11626	4.47856	9.00600
13	70.5	12.4	4.25562	2.51770	6.33884	10.71442
14	75.0	4.3	4.31749	1.45862	2.12757	6.29758
15	85.0	2.5	4.44266	0.91629	0.83959	4.07076
16	95.0	0.7	4.55388	-0.35318	0.12447	-1.60834
		Summation	68.23431	29.38014	90.45952	122.43589

$(\Sigma x^2)(\Sigma y) = 6172.4$

$(\Sigma x)(\Sigma xy) = 3597.2$

$(\Sigma x)(\Sigma y) = 2004.7$

$N \Sigma xy = 1959.0$

$N \Sigma x^2 = 1447.4$

$(\Sigma x)(\Sigma x) = 548.2$

$$\ln C = \frac{(\Sigma x^2)(\Sigma y) - (\Sigma x)(\Sigma xy)}{N \Sigma x^2 - (\Sigma x)(\Sigma x)} = \frac{6172.4 - 3597.2}{1447.4 - 863.2} = \frac{2575.2}{584.2} = 4.4081$$

$$C = 82.1 \simeq 82.0$$

$$n = \frac{(\Sigma x)(\Sigma y) - N \Sigma xy}{N \Sigma x^2 - (\Sigma x)(\Sigma x)} = \frac{2004.7 - 1959.0}{584.2} = \frac{45.7}{584.2} = 0.0782$$

$n = 0.078$

and the tool life relationship for the material is:

$VT_L^{0.078} = 82$.

APPENDIX B

VERIFICATION OF THE POSTULATED EFFECT OF THE SIZE OF THE CUT ON V_{60}

To verify that under the same cutting conditions, changing the size of the cut only:

$$V_{60}{}^{a} = V_{60}\, w^{1/3}\, t^{2/3} = \text{constant.}$$

A set of tool life tests were conducted on an AISI 1020 steel. The cutting velocity V_{60}, for t = 0.0057 in. and w = 0.050 in, was measured and predicted to be 160 fpm. Consequently for t = 0.0113 in. and w = 0.100 in the predicted V_{60} should be 80 fpm.

Figure 40 is a plot of the actual machining data for the heavier cuts. From this data the experimental value of V_{60} is found to be 85 fpm. The variation between the calculated and the experimental value of V_{60} is within the range expected due to experimental errors.

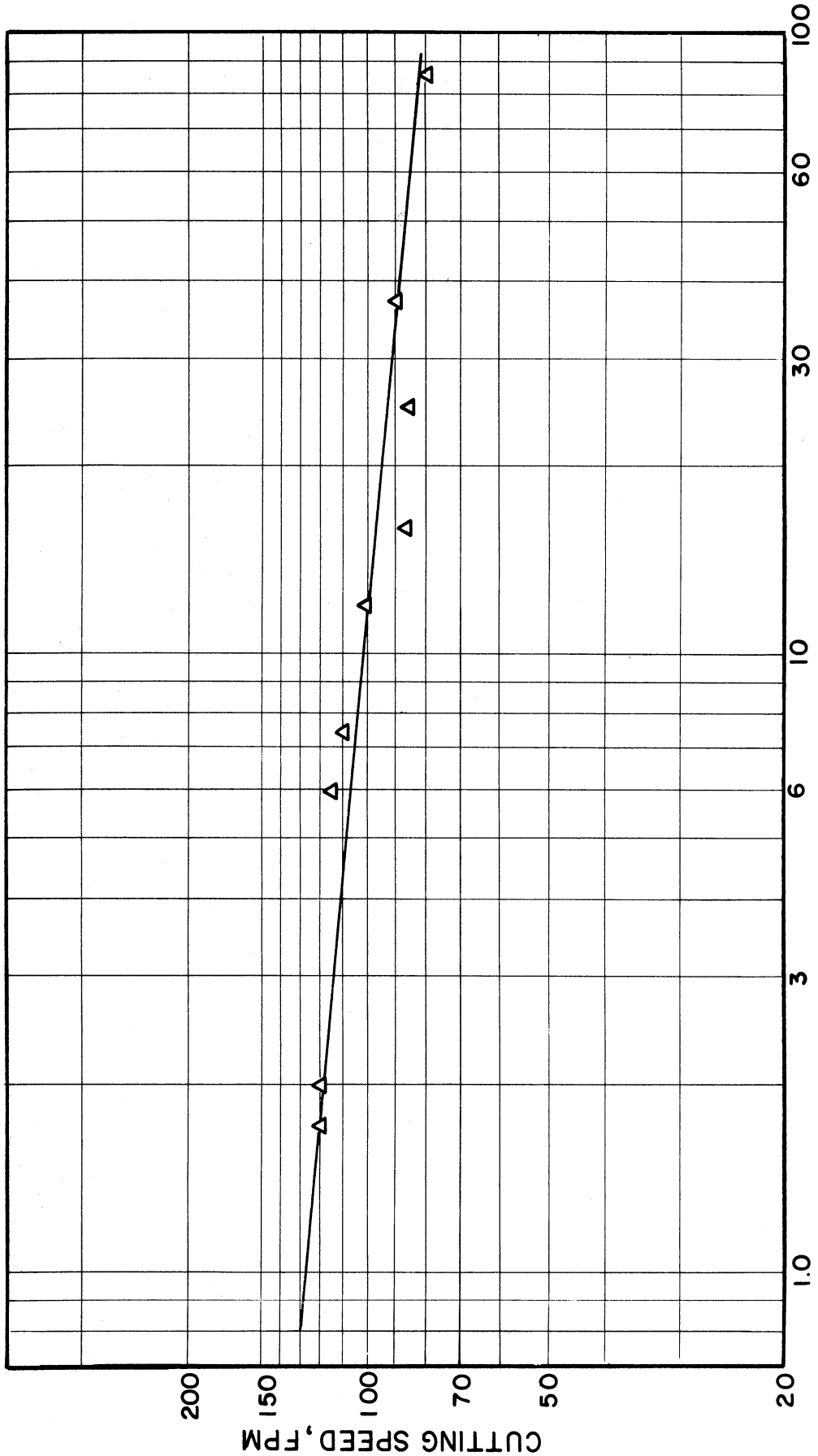

Figure 40. Cutting Speed Tool Life. AISI 1020 Steel.

BIBLIOGRAPHY

1. Ernst, H., "Physics of Metal Cutting", Machining of Metals, ASM, (1938).

2. ASM, Metals Handbook, 1, 8th Ed., (1961), 188.

3. Opitz, H., "Present-Day Status of Chip-Formation Research", Microtecnic, 14, (1960), 158-172.

4. Rumford, B., "An Inquiry Concerning the Source of Heat Which is Excited by Friction", Phil. Trans., Royal Society, 88, (1798), 278-287.

5. Cocquilhat, H., "Experiences sur la Resistance Utile Produites dans le Forage", Annales des Travaux Publics en Belgique, 10, (1851), 199.

6. Joessen, "Versuche ueber die guenstigste Form und Verwendung der Schneidwerkzeuge vom Standpunkte der Oeconomie der Betriebskraft", Z. Oesterreichischen Ingenieur und Architekten Vereins, (1865), 82-84.

7. Taylor, F. W., "On the Art of Cutting Metal", Trans. ASME, 28, (1907), 31-350.

8. Panchenko, K. P., Russkie Ucheniye Osnovopolozhniki Hauki O Rezanii Metallov, Mashgiz, Moscow (1952).

9. Timme, I. A., Soprotivlenie Metallov I Dereva Rezaniyu, St.Petersburg, (1870).

10. Timme, I. A., Memoirs sur le Rabotage des Metaux, St. Petersburg, (1877).

11. Tresca, H., "Memoirs sur le Rabotage des Metaux", Bulletin de la Societe d'Encouragement Pour L'Industrie Nationale, St. Petersburg, (1873).

12. Tresca, H., "On Further Applications of the Flow of Solids", Proc. Inst. Mech. Eng., (1878), 301.

13. Mallock, A., "The Action of Cutting Tools", Proc. Royal Society, 33, (1881), 127-139.

14. Piispanen, V., Teknillinen Aikakauslenti, 27, (1937), 315-322.

15. Merchant, E. M., "Mechanics of Metal Cutting Process", J. App. Phys., 16, (1945), 267-275 and 318-324.

16. Hartig, F., Versuche ueber Leistung und Arbeitsverbrauch der Werkzeugmaschinen, (1873).

17. Smith, R. H., Cutting Tools, England (1882).

18. Haussner, A.,"Das Hobeln von Metallen", Mitteilungen des Technischen Gewerbe Museums in Wien, No. 2, (1892), 117.

19. Reuleaux, "Ueber den Taylor White'schen Werkzeugstahl", Verein zur Befoerderung des Gewerbefleisses in Preussen, (1900), 179.

20. Finnie, I., "Review of the Metal-Cutting Analyses of the Past Hundred Years", Mech. Eng., August 1956, 715-718.

21. Beckett, C. A., "Report on the Present Status and Future Problems of the Art of Metal Cutting and Forming Metals", Mech. Eng., 46, (1923), 20-31, 57.

22. Kick, F., "Zur Folge der Wirkungsweise des Taylor White und des Bohler-Rapid-Stahles", Baumaterialkunde, 6, (1901), 227.

23. Brooks, J. F., "Photographs of Cutting Tools in Action", Proc. Inst. Mech. Eng., (1905), 365.

24. Rosenhain, W., "The Bearing of Microscopic Research on Iron and Steel Works Practice", Staffordshire Iron and Steel Institute, (April 1906), 83-99.

25. Briks, A.A., Rezanie Metallov (Stroganie), St. Petersburg,(1896).

26. Zvorikin, K. A., Rabota i Usilie, Neobkhodimie dlaya Otdelenaya Metallicheskikh Struzhek, Moscow, (1893).

27. Hermann, G., Section in "Lehrbuch der Ingenieur und Maschinen-mechanik", J. Weisbach, Editor, (1896), 865.

28. Linder, G., Book Review of Taylor's "Art of Metal Cutting", Z. VDI, 51, (1907), 1070.

29. Ernst, H. and Merchant, M. E., "Chip Formation, Friction and High Quality Machined Surfaces", ASM Symposium on Surface Treatment of Metals, (1941), 299-378).

30. Brackenburg, H. I., and Meyer, G. M., "The Heat Generated in the Process of Cutting Metal", Engineering, 91, (1911), 39-40.

31. Usacher, Y. G., Yavleniya Proiskhodyshchiya Pri Rezanii Metallov", Annales of the Peter the Great Polytechnic Institute of St.Petersburg, Russia, 23, (1915).

32. Shore, H., Metal Cutting Temperatures, Sc. D. Thesis, M.I.T., (1924).

33. Gottwein, K., "Die Messung der Schneidentemperatur beim Abdrehen von Flusseisen", Maschinenbau, 4, (1925), 1129-1135.

34. Herbert, E. G., "Measurement of Cutting Temperatures", Proc. Inst. Mech. Eng., I, (1926), 289-329.

35. Boston, O. W., and Gilbert, W. W., "Cutting Temperatures Developed by Single Point Turning Tools", Trans. ASM, 23, (1938), 703-726.

36. Schmidt, A. O., Boston. O. W., and Gilbert, W. W., "Measurements of Temperatures in Metal Cutting", Trans. ASME, 68, (1946), 47-49.

37. Chao, B. T., and Bisacre, G. H., "The Effect of Speed and Feed on the Mechanics of Metal Cutting", Proc. Inst. Mech. Eng., 165, (1951), 1-13.

38. Chao, B. T., and Trigger, K. J., "An Analytical Evaluation of Metal Cutting Temperatures", Trans. ASME, 73, (1951), 57-68.

39. Loewen, E. G., "Thermal Aspects of Metal Cutting," Dissertation M.I.T., (1952).

40. Coker, E.G., and Chakko, K. C., "Experiments on the Action of Cutting Tools", Proc. Inst. Mech. Eng., (1922), 567-621.

41. Coker, E. G., "Report on the Action of Cutting Tools", Proc. Inst. Mech. Eng., (1925), 357-434.

42. Schwerd, F., "Filmaufnahmen des Ablaufenden Spans bei ueblichen und bei sehr hohen Schnittgeschwindigkeiten", Z. VDI, 80, (1936), 233-236.

43. Ishii, S., "Macroscopic Kinematographs Applied to Research in Metal Cutting", World Engineering Congress, Tokyo, Paper 478, (1929).

44. Okochi, M., and Okoshi, M., "Researches on the Cutting Force", Tokyo Inst. of Phys. and Chem.Research, 5, (1927), 261-302.

45. Okoshi, M., "Researches on the Cutting Force, Part II, Action of the Planing Tool", Tokyo Inst. of Phys. and Chem. Research, 14, (1931), 193-225.

46. Okoshi, M., and Fukui, S., "Research on Cutting Action of Planing Tools", Tokyo Inst. of Phys. and Chem. Research, 455, (1933), 97-166.

47. Schwerd, F., "Neue Untersuchungen zur Schnitt-Theorie und Bearbeitsbarkeit", Stahl und Eisen, 51, (1931), 481-491.

48. Rapatz, F., "Das Oberflaechenaussehen bei der Spanabhebenden Bearbeitung insbesondere beim Drehen", Archiv fuer das Eisenhuettenwesen, 3, (1929-30), 717.

49. Ernst, H., and Martellotti, M., "The Formation and Function of the Built Up Edge", Mech. Eng., 57, (1953), 487-498.

50. Rosenhain, W., and Sturney, A. C., "Flow and Rupture of Metals During Cutting", Proc. Inst. Mech. Eng., (1925), 141-173.

51. Piispanen, V., "Theory of Formation of Metal Chips", J. Appl. Mech., 19, (1948), 876-881.

52. Field, M., and Merchant, M. E., "Mechanics of Formation of Discontinuous Chip in Metal Cutting", Trans. ASME, 71, (1949), 421-428.

53. Stabler, G. V., "The Fundamental Geometry of Cutting Tools", Proc. Inst. Mech. Eng., 165, (1951), 14-26.

54. Lee, E. H., and Shaffer, B. W., "The Theory of Plasticity Applied to a Problem of Machining", J. Appl. Mech., 18, (1951), 405-413.

55. Lee, E. H., "A Plastic Flow Problem Arising in the Theory of Discontinuous Machining", Trans. ASME, 76, (1954), 189-194.

56. Hucks, H., "Plastizitaetsmechanische Grundlagen und Kenngroessen der Zerspannung", Dr. Ing. Dissertation, Aachen, (1951).

57. Hucks, H., "Plastizitaetsmechanische Theorie der Spanbildung", Werkstatt und Betrieb, 85, (1952), 1-6.

58. Shaw, M. C., Cook, N. H., and Finnie, I., "The Shearing Angle Relationship in Metal Cutting", Trans. ASME, 75, (1953), 273-288.

59. Cook, W. H., Finnie, I., and Shaw, M. C., "Discontinuous Chip Formation", Trans. ASME, 76, (1954), 153-188.

60. Hill, R., "The Mechanics of Machining: A New Approach", J. Mech. Phys. Solids, 3, (1954), 47-53.

61. Okushima, K., and Hitomi, K., "On the Cutting Mechanism for Soft Metals", Memoirs Faculty of Eng., Kyoto University, 19, (1957), 135-166.

62. Okushima, K., and Hitomi, K., "An Analysis of the Mechanism of Orthogonal Cutting", Memoirs, Faculty of Eng., Kyoto University, 20, (1958), 95-116.

63. Lamm, M. M., "Chip Formation in Metal Cutting; a Hydrodynamic Theory", Engineering, (1959), 444-446.

64. Lamm, M. M., Osnovi Gidrodinamicheskoi Teoria Pezania Metallov, Russia, (1940).

65. Colding, B. N., "A Yield Criterion Applied to the Shear Angle Relationship", Microtecnic , 14, (1960), 47-60.

66. Loladze, T. N., Iznos Rezhushchevo Instrumenta, Mashgiz, Moscow, (1958).

67. Zorev, N. N., Voprosii Mechaniki Protsessa Pezaniya Metallov, Mashgiz, Moscow, (1956).

68. Boulger, F. W., Shaw, H. L., and Johnson, H. E., "Constant Pressure Lathe Test for Measuring the Machinability of Free Cutting Steels", Trans. ASME, 71, (1949), 431-446.

69. Merchant, M. E., Ernst, H., and Krabacher, E. J., "Radioactive Cutting Tools for Rapid Tool Life Testing", Trans. ASME, 75, (1953), 549-559.

70. Schlesinger, G., "Machinability of Metals", The Tool Engineer, 17, (Jan. 1947), 18-27.

71. Janitzky, E. J., "Taylor Speed and Its Relation to Reduction of Area and Brinell Hardness", Trans. ASM, 26, (1938), 1122-1131.

72. Janitzky, E. J., "Machinability of Plain-Carbon, Alloy, and Austenitic (Nonmagnetic) Steels, and Its Relation to Yield-Stress Ratios when Tensile Strengths are Similar", Trans. ASME, 66, (1944), 649-652.

73. Langenbach, F., "Die Zerspannbarkeit - Kennziffer V_{60} in ihrer Beziehung zur Zugfestigkeit und Streckgrenze beim Schrupp-Dreh Vorgang vonlegierten und unlegierten Staehlen", Dr. Ing. Dissertation, Aachen, (1932).

74. Boston, O. W., and Colwell, L. V., "The Effect of Hardness on the Machinability of Six Alloy Steels", Trans. ASM, 31, (1943), 955-979.

75. Schlesinger, G., "Brinell Hardness Does Not Measure Machinability", American Machinist, 91, (July 1947), 125-136.

76. SAE Tech. Committee on Iron and Steel, "Types of Steel, Microstructure, Chem. Composition and Tool Compatibility", SAE Jour., 62, (1954), 47-53.

77. United States Air Force Machinability Report No. 2., Curtis Wright Corporation, Wood Ridge, New Jersey, (1951).

78. Bridgman, P. S., "The Stress Distribution at the Neck of a Tension Specimen", Transaction ASM, 32, (1944), 553-574.

79. Meyer, E., "Untersuchungen ueber Haertepruefung und Haerte", Z. VDI, 52, (1908), 645-654, 740-748, and 835-844.

80. Lightner, M. W., and Herty, C. H., Jr., "The Traverse Impact Strength of Plain Carbon, Normalized Steels", Cooperative Bulletin 59, Carnegie Inst. Tech. and Min. and Met. Advisory Boards, (1932).

81. Howard, R. T., and Cohen, M., "Quantitative Metallography by Point-Counting and Lineal Analysis", Trans. AIME, 172, (1947), 413-426.

82. Bain, E. C., Functions of the Alloying Elements in Steel, ASM, Cleveland, (1939).

83. Reichel, W., "Abgekuerztes Standzeitmittlungs Verfahren fuer Spangebende Werkzeuge", Maschinenbau, 11, (1932), 473-478.

84. Colwell, L. V., A Method for Studying the Behavior of Cutting Fluids in Wear of Tool Materials, University of Michigan, Industry Program, I.P. 225, (1957).

85. Timoshenno, S., and Goodier, N. J., Theory of Elasticity, McGraw Hill Book Company, Inc., New York, (1951).

86. Love, A. E. H., A Treatise on the Mathematical Theory of Elasticity, Cambridge University Press and Dover Publication, New York, (1944).

87. Hertz, H., J. F. Math. (Crelle), 92, Germany (1881).

88. Reichenbach, G. S., "Experimental Measurement of Metal Cutting Temperature Distributions", Trans. ASME, 80, (1958), 525-540.

89. Bridgman, P. S., Dimensional Analysis , Yale University Press, New Haven, (1935).

90. Buckingham, E., Phys. Rev., 4, (1941), 345.

91. Herbert, E. G., "Cutting Tools Research Committee. Report on Machinability", Proc. Inst. Mech. Eng.,(1928), 775-825.

92. Tabor, D., The Hardness of Metals, Oxford (1951).

93. Schmidt, A. O., Heat in Metal Cutting, Chapter in Machining Theory and Practice, ASM, (1950).

94. Pahlitzsch, G., and Helmerdig, H., "Das Temperaturfeld am Drehmeissel waermetechnisch betrachtet", Z. V.D.I., 87, 564-571.

95. Danielian, A. M., Teplota i Iznos Instrumentov v Protzesse Rezania Metallov, Mashgiz, (1954).

96. Vieregge, G., "Die Energiverteilung und die Temperatur bei der Zerspanung", Werkstatt und Betrieb, 86, (1943) 691-703.

97. Shaw, M. C., Cook, H., and Finnie, I., "Shear-Angle Relationship in Metal Cutting", Trans. ASME, 75, (1953), 273-288.

98. Keceioglu, D., "Shear Strain Rate in Metal Cutting and Its Effect on Shear Flow Stress", Trans. ASME, 80, (1958), 158-168.

99. Drucker, D. C., "A Dimensional Analysis of Metal Cutting", J. Appl. Phys., 21, 104-107, (1950).

100. Shaw, M. C., Metal Cutting Principles, 3rd Ed., M.I.T., (1954).

101. Kronenberg, M., Grundzuege der Zerspanungslehre, Springer, (1954).

102. Shaw, M. C., et al., Machining Titanium, M.I.T. (1954).

103. Bisacre, F.F.P., and Bisacre, G. H., "The Life of Carbide-Tipped Turning Tools", Proc. Inst. Mech. Eng., War Emergency Issue No.35, 157, (1947), 452-469.

104. Chao, B. T., Trigger, K. J., and Zylestra, L. B., "Thermophysical Aspects of Metal Cutting", Trans. ASME, 74, (1952) 1039-1054.

105. Woxen, R., "A Theory and an Equation for the Life of Lathe Tools", Ingenioersvetenskapsakademiens Handligar, Nr. 119, (1932).

106. Boston, O. W., Metal Processing, 2nd Ed., J. Willy and Sons, Inc., New York (1951), 147.

107. Merchant, M. E., and Ernst, H., "Principles of Metal Cutting and Machinability", Section 17 of the Tool Engineer's Handbook, 1st Ed., (1949), 324-326.

108. ASME, Manuel on Cutting of Metals, 2nd Ed., (1952), 302-303.